HEAT EXCHANGER DESIGN AND TESTING FOR A 6-INCH ROTATING DETONATION ENGINE

THESIS

Scott W. Theuerkauf, 2nd Lieutenant, USAF

AFIT-ENY-13-M-33

DEPARTMENT OF THE AIR FORCE
AIR UNIVERSITY

AIR FORCE INSTITUTE OF TECHNOLOGY

Wright-Patterson Air Force Base, Ohio

APPROVED FOR PUBLIC RELEASE; DISTRIBUTION UNLIMITED

The views expressed in this thesis are those of the author and do not reflect the official policy or position of the United States Air Force, Department of Defense, or the United States Government. This material is declared a work of the U.S. Government and is not subject to copyright protection in the United States.

AFIT-ENY-13-M-33

HEAT EXCHANGER DESIGN AND TESTING FOR A 6-INCH ROTATING DETONATION ENGINE

THESIS

Presented to the Faculty

Department of Aeronautics and Astronautics

Graduate School of Engineering and Management

Air Force Institute of Technology

Air University

Air Education and Training Command

In Partial Fulfillment of the Requirements for the

Degree of Master of Science in Aeronautical Engineering

Scott W. Theuerkauf, BS

2nd Lieutenant, USAF

March 2013

APPROVED FOR PUBLIC RELEASE; DISTRIBUTION UNLIMITED

AFIT-ENY-13-M-33

HEAT EXCHANGER DESIGN AND TESTING FOR A 6-INCH ROTATING DETONATION ENGINE

Scott W. Theuerkauf, BS

2nd Lieutenant, USAF

Approved:

Paul I. King (Chairman)	Date
Fred Schauer (Member)	Date
Jeremy S. Agte, Lt Col, USAF (Member)	Date

AFIT-ENY-13-M-33

Abstract

This thesis explains the design and testing of a water-cooled rotating detonation engine (RDE) run on hydrogen and air. The change in water temperature as it cooled the engine was used to find the steady heat rate into the containing walls of the detonation channel. The engine successfully ran four times for 20 seconds each. The steady-state heat rate was measured to be 2.5% of the propellant lower heating value (LHV) into the outer wall and 7.1% of LHV into the inner wall. Additionally, a quick-response resistance temperature detector (RTD) was used in an uncooled RDE of similar dimension to the cooled RDE to estimate the transient heat flux profile in the detonation channel. The average heat flux into the outer wall near the base of the channel was measured to be four times greater than the average heat flux over the entire cooled wall at steady-state, indicating the heat flux decreases significantly with axial distance. In addition, the large difference in heat absorption between the inner and outer cooled walls indicates that the heat flux into the inner wall is greater than that into the outer wall.

Acknowledgments

I would like to thank Dr. Paul King for giving me the opportunity to research this topic. I found great satisfaction in experiencing both design and experimentation during this thesis and recognize that few graduate students have the opportunity to do both.

I would also like to thank Dr. Fred Schauer for inviting me to conduct this research at the Detonation Engine Research Facility and for giving me an opportunity to work with everyone there. I would further like to thank Dr. John Hoke whose years of experience helped ensure my experiments were done in a safe, cost-effective, and timely manner.

Without the help of Richard Anthony and Rob Free with the Turbine Research Facility, I would not have been able to include the heat flux gauge with this research. Rich's knowledge of signal processing and thin film gauges and Rob's assistance in preparing and repairing the heat flux gauges have been critical to its success so far.

I am indebted to Andrew Naples for double-checking my design calculations, providing his experience with cooling the 3-inch RDE, and for providing technical expertise in regard to the RDE control programs.

Curtis Rice and Justin Goffena were instrumental in fabricating and assembling the electronics, components, and structures necessary for this research. I would not have been able to test without their help.

I would like to thank Rachel Russo, Chris Stevens, and Capt Robert Fievesohn for their assistance throughout this research project. Their explanations of RDE behavior, instrumentation techniques, and concurrent research as well as their direct help in data acquisition were invaluable.

Finally, I would like to thank my family and friends for supporting me during this period and enduring my many attempts to explain my thesis topic in layman's terms.

TABLE OF CONTENTS

Page

Abstract iv
Acknowledgments v
TABLE OF CONTENTS vi
LIST OF FIGURES viii
LIST OF SYMBOLS x
CHAPTER 1. INTRODUCTION 1
1.1 Differences between Pulsed and Rotating Detonation Engines 1
1.2 Research Objectives 3
1.3 Preview 3
CHAPTER 2. LITERATURE REVIEW 4
2.1 Pratt and Whitney 3-inch RDE Water-Cooling Research 4
2.2 AFRL 6-inch RDE Research 6
2.3 Using Resistance Temperature Detectors to Find Heat Flux 9
CHAPTER 3. METHODOLOGY AND TEST SETUP 11
3.1 Water-Cooled RDE Design 11
3.2 Deviations from the Design 20
3.3 Cooled RDE Experimental Setup 22
3.4 Cooled RDE Testing Procedure 26
3.5 Heat Flux Gauge in the Uncooled RDE 29
3.6 Uncooled RDE Test Setup 32
CHAPTER 4. RESULTS AND DISCUSSION 34
4.1 Cooled RDE Operating Point 34

4.2 Steady-State Heat Rate 34

4.3 Design Lessons Learned 37

4.4 Low Equivalence Ratio Runs in the Cooled RDE 39

4.5 Heat Flux Gauge Results 41

4.6 Comparison 47

CHAPTER 5. CONCLUSIONS AND RECOMMENDATIONS 49

5.1 Conclusions 49

5.2 Recommendations for Future Water-Cooled RDE Research 50

5.3 Recommendations for Future Heat Flux Gauge Research 52

APPENDIX A. 20-SECOND COOLED RDE RUNS 54

APPENDIX B. COOLED RDE REASSEMBLY 59

REFERENCES 65

LIST OF FIGURES

Page

Figure 1. Unrolled rotating detonation wave from high-speed video (4) 2

Figure 2. Cooled 3-inch Pratt and Whitney RDE 4

Figure 3. Comparison of 6-inch RDE and 3-inch RDE normal operating maps (2) 7

Figure 4. 6-inch RDE components (6) 8

Figure 5. Water-Cooled RDE design 11

Figure 6. Original cooled RDE design cross-section model 18

Figure 7. Stainless steel outer body containing wall after two-second operation..... 21

Figure 8. Aft end of fully assembled water-cooled RDE after all modifications 22

Figure 9. Fore end of fully assembled water-cooled RDE..... 23

Figure 10. Cooling water ports for the RDE center body with thermocouple visible 25

Figure 11. Low-speed capture of detonation in the cooled RDE..... 28

Figure 12. Low-speed capture of deflagration from the cooled RDE..... 28

Figure 13. Sensing face of the heat flux gauge 30

Figure 14. Heat flux gauge with protective cover and potting material removed 30

Figure 15. Heat flux gauge non-dimensionalized resistance vs. temperature..... 31

Figure 16. Modified 6-inch RDE used for heat flux gauge testing..... 32

Figure 17. Failed gland seal design for outer body wall..... 38

Figure 18. Air mass flow rate and equivalence ratio over time during a 2s run..... 39

Figure 19. Comparison of detonation exhaust plumes at equivalence ratios of 1.05 (top) and 0.84 (bottom) 40

Figure 20. Heat flux gauge before and after data collection..... 41

Figure 21. Wall temperature in the first 43ms of RDE operation..... 42

Figure 22. Heat flux, temperature, and PCB pressure during startup 43

Figure 23. FFT distribution of wave velocities measured from PCB pressure rises 44

Figure 24. Heat flux, temperature, and PCB pressure after 38 ms 46

Figure 25. Average heat flux into the gauge..... 47

LIST OF SYMBOLS

Acronyms

AFRL	Air Force Research Laboratory
DERF	Detonation Engine Research Facility
HHV	Higher heating value
LHV	Lower heating value
PDE	Pulsed detonation engine
RDE	Rotating detonation engine
RTD	Resistance temperature detector
RTV	Room temperature vulcanization
TRF	Turbine Research Facility

Symbols	[SI units] {English units}
A	area
c_p	constant pressure specific heat [J/(kg*K)] {BTU/(lbm*R)}
D_h	hydraulic diameter [m] {in}
f	Darcy friction factor
h	convective heat transfer coefficient [W/(m^2*K)] {BTU/(ft^2*R)}
H	cylindrical wall height [m] {in}
k	thermal conductivity [W/(m*K)] {BTU/(ft*R)}
$\dot{m}$	mass flow rate [kg/s] {lbm/min}
Nu	sample standard deviation
P	pressure [Pa] {psi}
P_c	cross-section perimeter [m] {in}
Pr	Prandtl number
q	heat release [W] {BTU}
q”	heat flux [W/m^2] {BTU/ft^2}
r	radius [m] {in}
Re	Reynolds number
t	wall thickness [m] {in}
T	temperature [K, C] {R, F}
u	velocity [m/s] {ft/s}

Greek Symbols	[SI units] {English units}
α_R	coefficient of thermal resistivity [1/K] {1/R}
ε	roughness factor
μ	viscosity [(N*s)/m^2] {(lbf*s)/in^2}
π	ratio of a circle’s circumference to its diameter
σ_h	hoop stress [MPa] {ksi}

Subscripts

0	reference
c	cross-section
D	for flow through a pipe of diameter D

Subscripts (continued)

f	fluid
in	at the entrance of the heat exchanger
m	mean
out	at the exit of heat exchanger
s	surface
sd	surface against detonation
sw	surface against water
w	wall

HEAT EXCHANGER DESIGN AND TESTING FOR A 6-INCH ROTATING DETONATION ENGINE

CHAPTER 1. INTRODUCTION

Pressure gain combustion is the focus of much recent research due to the theoretical improvement in efficiency over traditional deflagration engines. The defining characteristic of pressure gain combustion is the use of detonation waves to combust propellants, increasing stagnation temperature and pressure of the reactants while deflagration increases temperature with a slight loss in stagnation pressure. The various forms of pressure gain combustion differ in their manipulation of detonations. Two of these forms of particular interest to the combustion community are pulse detonation engines (PDEs) and rotating detonation engines (RDEs).

1.1 Differences between Pulsed and Rotating Detonation Engines

The primary difference between PDEs and RDEs is in how each uses detonation waves to combust propellants. In PDEs the detonation wave travels down the length of a tube. Between each detonation, the exhaust products must be expelled and fresh reactants injected into the tube, decreasing the amount of operating time consisting of actual combustion and greatly varying the exhaust velocity, temperature, and pressure (1). This process also requires moving parts to sequentially meter in air and fuel and stop injection during detonation. Meanwhile, RDEs manipulate an annular injection channel

and propellant flow rates in such a way that a single detonation wave fired into the channel travels continuously around the base of the channel. As the wave passes, fresh reactants enter behind it so that by the time the detonation wave travels the circumference of the channel enough reactants have refilled to sustain the wave. Fig. 1 shows luminosity of the detonation travelling in a clear-wall RDE. Because the purge and fill cycles are absent in an RDE, RDE design requires no moving parts, significantly reducing complexity. In addition, the exhaust is much steadier than that of a PDE (2, 3).

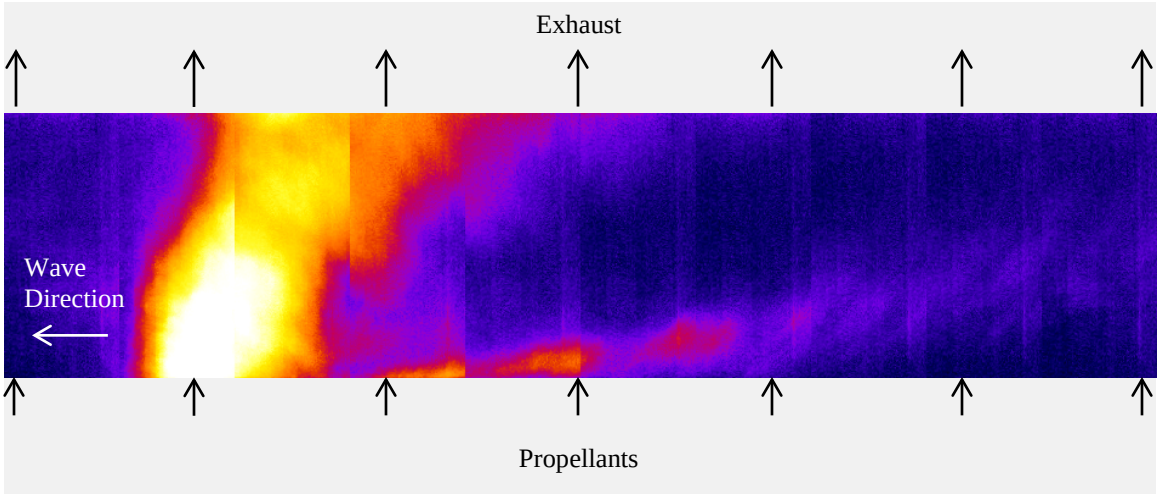

Figure 1. Unrolled rotating detonation wave from high-speed video (4)

Another difference that plays an important role in heat transfer is operating frequency. While detonations may pass a point in a PDE tube on the order of 10 to 100 times per second, the wall of a 6-inch RDE may be heated by detonation waves more than 3000 times per second (2). The result is that RDEs heat much faster and reach higher temperatures than PDEs (5). While PDEs can run continuously needing no more than free convection and radiation to avoid overheating, RDEs are typically limited to

less than one second of runtime without an active cooling system (2, 3). If RDEs are to be used continuously they need to be engineered with the expected heat transfer in mind.

1.2 Research Objectives

This research sought to quantify the heat transfer to both the inner and outer containing walls of an RDE. In particular, steady state heat transfer was measured in a water-cooled RDE and compared with short-run wall heat flux data collected by a resistance temperature detector (RTD). The RTD can show the waveform of the heat flux into the outer wall of the RDE during a period of steady operation.

1.3 Preview

Chapter 2 discusses previous research done on RDEs, cooling them, and using RTDs to quantify heat transfer on turbine blades at very small timescales. Chapter 3 illustrates the design and setup of test equipment and procedures used in testing. Chapter 4 covers the results and analysis of the experimentation. Finally, chapter 5 provides conclusions of the experiment and recommended future work in this area of research.

CHAPTER 2. LITERATURE REVIEW

2.1 Pratt and Whitney 3-inch RDE Water-Cooling Research

One of the RDEs operated by AFRL in the Detonation Engine Research Facility (DERF) is a 3-inch diameter RDE on loan from Pratt and Whitney, Seattle Aerosciences Center (Fig. 2) (3). This engine has been used to test different fuel mixtures and to study RDE exhaust steadiness among other topics. Of interest to this paper is the work done in water-cooling (5).

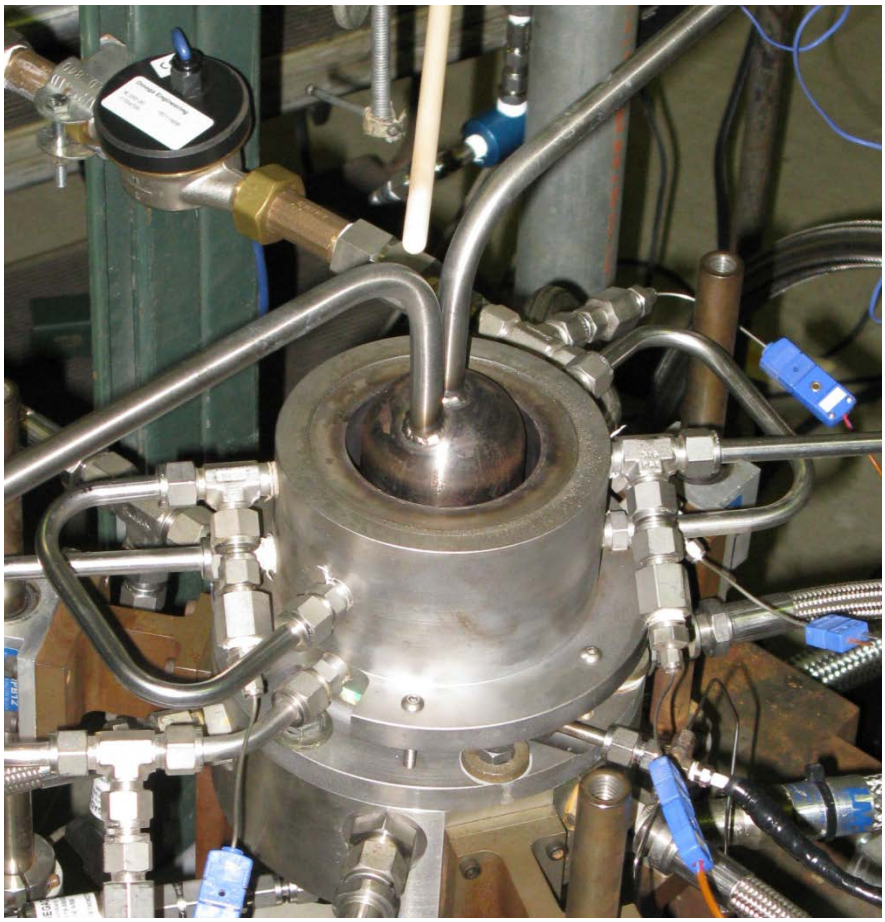

Figure 2. Cooled 3-inch Pratt and Whitney RDE

The outer body of this RDE was replaced with a water jacket designed to stay cool by routing water circumferentially around the detonation channel. The original center body was also replaced with a water jacket that had water travel down through the inside of the center body, then spread out against the walls and flow axially along the detonation channel to the exit. For both the center body and the outer body the temperature of the water was measured before and after it entered the RDE. With the mass flow rates into each water jacket, these could give total heat deposit rate into the water from the RDE. This was compared with lower heating value (LHV) of the flow (5).

The cooled 3-inch RDE was run for 60 seconds, once at 30.2 lb/min and once at 25.4 lb/min, both at an equivalence ratio of 2.0. Both used hydrogen as the fuel and a mixture of nitrogen and 22.7% oxygen to simulate air. In both tests the outer body water jacket extracted about 5.5% of the flow LHV while the center body water jacket extracted around 8%. One problem with cooling the center body was that the water supply lines crossed over the RDE exhaust (as seen in Fig. 2), increasing the total heat deposit rate into the water sent to the center body. This could explain why the center body saw more heat transfer than the outer body (5).

Another problem with this design is that the outer body is only partly cooled. The base of the outer body was left uncooled to allow the pre-detonator to be placed in the conventional position. This meant more reliable ignition of the engine, but the lack of cooling did not allow the RDE to run to complete thermal equilibrium. It also means that some of the heat lost to the outer body did not make its way to the water jacket under

thermal equilibrium. Thermal equilibrium in this case is restricted only to the water jacket, not the RDE as a whole (5).

This experiment was very influential in the design of the water-cooled 6-inch RDE. It not only gave the expected heat rate into each wall, but also provided examples on water jacket patterns, warned to account for thermal expansion, and indicated that the bottom of the outer body near the base of the detonation channel would absorb less heat than elsewhere in the channel. While the last point proved to be a misleading assumption, the others were necessary to designing an RDE for continuous operation.

2.2 AFRL 6-inch RDE Research

In 2011 AFRL built a new RDE. This one featured a modular design to enable full modification of every dimension of the RDE and did not include any proprietary designs. The engine was designed and built at the DERF and was successfully tested over a wide range of mass flow rates and equivalence ratios for hydrogen-air mixtures and was shown to operate normally in an equivalence ratio range lower than for the 3-inch RDE (Fig. 3). It has since been used to investigate the effects of back-pressurization on detonability, the use of ethylene instead of hydrogen, and many other basic RDE research topics (2).

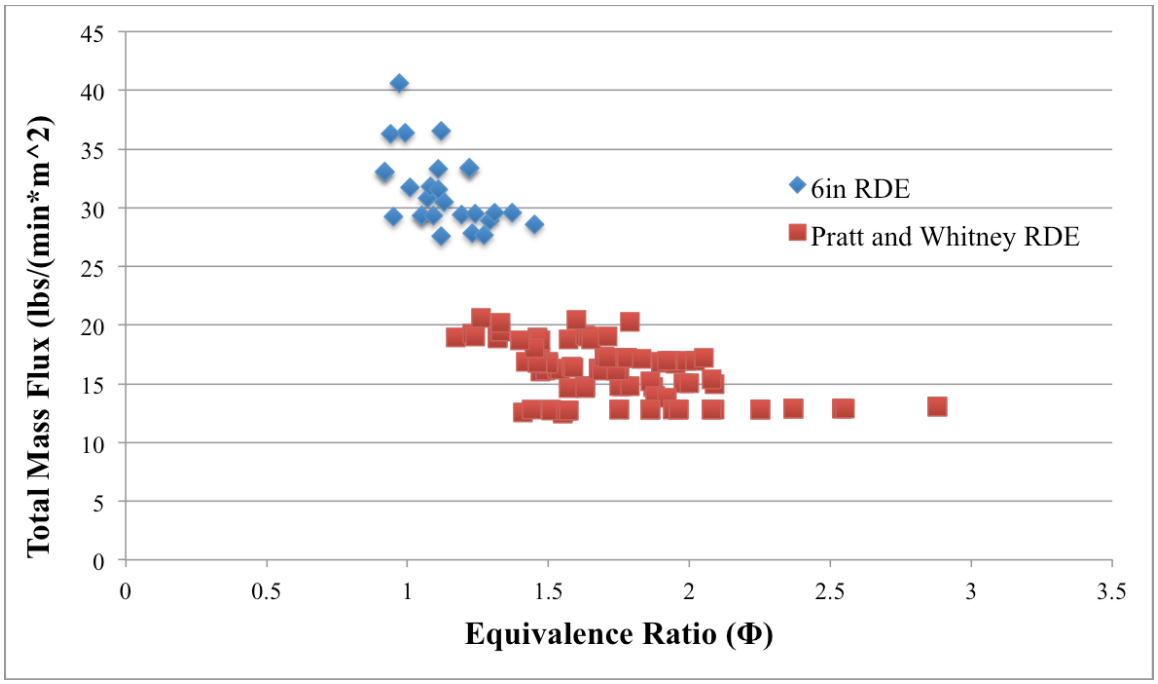

Figure 3. Comparison of 6-inch RDE and 3-inch RDE normal operating maps (2)

RDE operation is seldom as orderly as theory understands it. As such, there were three operational modes observed in the 6-inch RDE: steady, bifurcation, and reversal. In steady operation, the detonation wave travels in one direction around the channel and maintains relatively constant velocity. Bifurcation involves two waves parting in opposite directions and travelling around the channel to meet again at the opposite side. Bifurcation occurs at startup as the detonation wave from the pre-detonator transitions to steady operation, but steady operation can also destabilize back into a bifurcation. In a reversal mode, the detonation wave stops in the middle of the channel and resumes steady operation but in the opposite direction (2).

The detonation channel of the vertically-mounted 6-inch RDE had a 6.06” outer diameter and 5.46” inner diameter with a height of 5”. Air entered the base of the

channel through a 0.125” gap. The oxidizer manifold was fed radially by five 1-inch hoses that blew directly into the channel. Hydrogen entered the channel through eighty evenly spaced 0.10” diameter holes. The manifold beneath these holes was fed from underneath by a 1” tube centered in the fuel manifold. This setup made for an even distribution of fuel into the detonation channel. The modular components of the RDE are shown below in Fig. 4.

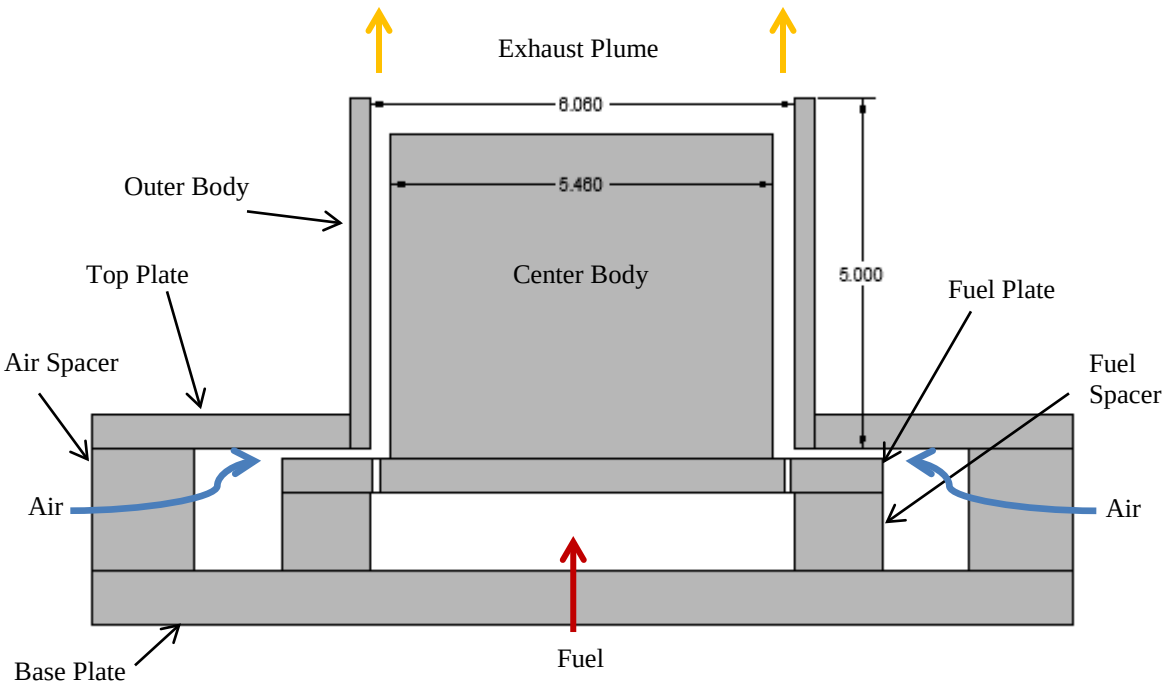

Figure 4. 6-inch RDE components (6)

One of the issues with the 6-inch RDE is that it is mounted vertically. This makes assembly very simple, since all parts stack on one another, but it means the exhaust is directed at the ceiling of the test cell. This is mitigated by blowing cool mixing air above

the exhaust plume, but without an exhaust door on the ceiling, the vertical orientation prohibits the engine from running continuously, regardless of how well it is cooled.

Because the operational environment is well known and there are no proprietary designs on the 6-inch RDE, it was used as a starting point for the water-cooled RDE. The primary deviation from the 6-inch RDE design was increasing the fuel manifold feed lines from one to four, which modified the flow pattern entering the detonation channel. All other modifications had little to no effect on the flow entering the detonation channel.

2.3 Using Resistance Temperature Detectors to Find Heat Flux

RTDs offer the opportunity to quantify heat flux to a surface over very short time steps. RTDs work by exploiting platinum's ability to change resistance very linearly based on changes in temperature. Specifically, the difference between the resistance R at a temperature T and the reference resistance R_0 at the reference temperature T_0 is linearly related to R_0 and the thermal resistivity coefficient α_R (Eq. 1).

$$\frac{R-R_0}{R_0} = \alpha_R(T - T_0) \tag{1}$$

If constant current is assumed, the resistance terms may be replaced with voltage terms. While this equation applies for many materials, platinum is the preferred metal for RTDs because the thermal resistivity coefficient remains nearly constant over a broad range of temperatures.

The Turbine Research Facility (TRF) at AFRL has used this property with platinum circuits to place unobtrusive high-density sensor arrays on turbine blades with

quick response times on the order of 200 kHz. This speed was possible by keeping the platinum thickness to ~40 nm. However, the primary goal of that research was not to measure the temperature as much as to understand the transient heat flux profile entering turbine blades (7).

The heat flux through a semi-infinite solid required to give a varying temperature profile is impossible to calculate analytically. There are, however, analytical solutions to temperature profiles based on step inputs in heat flux. By modeling the complex temperature profile as a combination of simple temperature profiles, a discrete heat flux can be derived. On the fundamental level, this is how the TRF derived heat flux profiles from RTDs (8).

On a more sophisticated level, the heat flux was modeled as a convolution of the temperature on the gauge and a transfer function specific to the instrumentation. While two different gauges will have two different transfer functions, the transfer function for any temperature profile on one gauge will remain the same (8). This means that by assuming the gauge acts as a semi-infinite solid for the purposes of heat transfer, simple well-known solutions can be used to find an RTD's transfer function which remains the same even under complex heat profiles. This methodology was applied to the 6-inch RDE to find the heat flux at a point on the outer body wall using a single RTD.

CHAPTER 3. METHODOLOGY AND TEST SETUP

3.1 Water-Cooled RDE Design

In order to avoid routing the water into the center body through the exhaust, a cooled RDE needed to be a completely new engine (Fig. 5). The detonation channel dimensions and air manifold from the 6-inch RDE were maintained in an attempt to keep the operating space as similar as possible, but the fuel manifold was modified to allow water to flow in and out of the cooling body through the fore of the engine. Additionally, the fuel manifold and center body were designed to slip into and out of the air manifold and outer body to allow easier adjustment of the air inlet gap than on the 6-inch RDE. For this experiment, the gap was maintained at 0.125 inches.

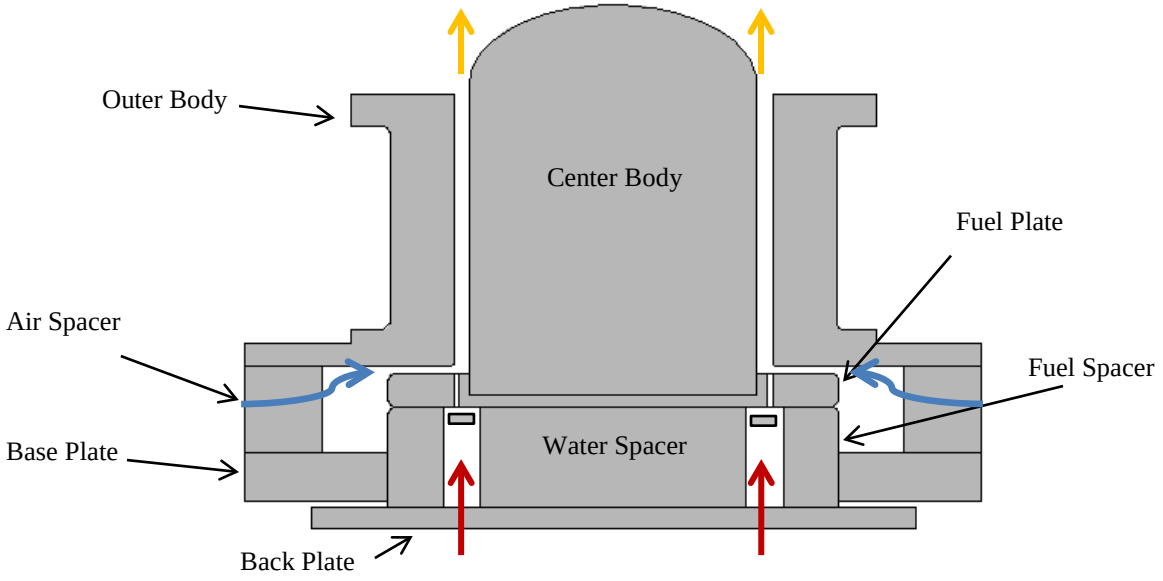

Figure 5. Water-Cooled RDE design

Designing the cooling system started with an assumption that the outer body and the center body would absorb heat at the same rate. The total heat rate into each was assumed to be 5% of the available enthalpy. This was lower than the recorded heat percentage absorbed by the 3-inch RDE, but was assumed since the 6-inch RDE was shorter relative to its diameter than the 3-inch RDE (5). The total available enthalpy for combustion inside the channel was assumed to be the maximum enthalpy increase from the complete reaction of the hydrogen and air, also called the higher heating value (HHV). This is calculated by subtracting the total standard enthalpy of the reactants and subtracting that from the total standard enthalpy of the products. The HHV is the higher value because it computes the standard enthalpy of liquid water, so it includes the heat released to condense all water from gaseous form (9).

A commonly used operating point on the 6-inch RDE that usually successfully detonated was at an air mass flow rate of 175 lb/min and an equivalence ratio of 1.0 (2). The HHV for this mixture is 5.35MW, so a heat transfer rate of 268kW into each wall was assumed for the purpose of initial design.

There were two goals in designing the water jackets: to stop water from boiling in the channels and to stop the walls from overheating. Boiling absorbs more heat from the wall, but detracts from the convection downstream of the boiling point and reduces the accuracy of the temperature gauge at the water jacket outlet (10). The total increase in mean water temperature T_m for an expected heat rate q and mass flow rate $\dot{m}$ and variable specific heats c_p was calculated using conservation of energy (Eq. 2).

$$q = \dot{m}\left[\left(c_p \cdot T_m\right)_{in} - \left(c_p \cdot T_m\right)_{out}\right] \tag{2}$$

Even with small changes in mean temperature, the water near the hot surfaces of the containing walls could still boil even if the mean temperature were low (10). This was prevented by increasing the convective heat transfer of the water in the channel. Convection is described by Newton's Law of Cooling, which relates convective heat flux q'' to a fluid's temperature gradient by the convection heat transfer coefficient, h (Eq. 3) (10).

$$q'' = \frac{q}{A_{sw}} = h(T_{sw} - T_m) \tag{3}$$

During design the heat flux was assumed to be constant over each surface so that heat flux was simply the heat rate q divided by the transfer area, A_{sw}. Thus, for a given heat flux, the difference between the fluid mean temperature T_m and the surface temperature T_{sw} can be decreased by increasing h. The convective heat transfer coefficient is in turn a function of the flow field. Several studies have found empirical formulas for non-dimensional Nusselt numbers, related to h by Eq. 4 (10).

$$h = \frac{k_f}{D_h} Nu_D \tag{4}$$

Non-circular tubes can be modeled as circular tubes with a hydraulic diameter D_h based on the tube cross-section area A_c and perimeter P_c (Eq. 5) (10).

$$D_h = \frac{4A_c}{P_c} \tag{5}$$

The final design indicated a Reynolds number calculated by Eq. 6 to be on the order of 10^5 for both the outer body and center body cooling channels.

$$Re_D = \frac{\rho u_m D_h}{\mu_f} = \frac{\dot{m} D_h}{\mu_f A_c} = \frac{4\dot{m}}{\mu_f P_c} \tag{6}$$

Reynolds number relates mass flow rate $\dot{m}$ through the channel to the flow viscosity μ_f and cross-sectional perimeter P_c. Thus, while laminar solutions were included during the design process, the Nusselt numbers used for each final design were calculated using Gnielinski's equation (Eq. 7), which holds for Reynolds numbers between 3000 and $5*10^6$ and Prandtl numbers between 0.5 and 2000 (10). This approximation assumes fully developed flow even though the outer body channel is too short for fully developed flow and the center body only has fully developed flow for roughly 10% of the channel length, but the assumption is valid for the purposes of design since turbulent fully developed flow has a lower heat transfer rate than in the entry length.

$$Nu_D = \frac{(f/8)(Re_D - 1000)Pr}{1 + 12.7(f/8)^{1/2}\left(Pr^{2/3} - 1\right)} \tag{7}$$

Finally, the Darcy friction factor *f* was calculated using S.E. Haaland's approximate explicit solution (Eq. 8) to the Colebrook equation (11).

$$f \approx \left\{-1.8 \log\left[\frac{6.9}{Re_D} + \left(\frac{\varepsilon/D_h}{3.7}\right)^{1.11}\right]\right\}^{-2} \tag{8}$$

This calculation not only enabled a more direct analytical approach to designing the cooling jackets, it also allowed surface roughness (ε) to be factored into the Nusselt number calculations. Since increasing roughness can only improve heat transfer until *f* is roughly four times that of smooth walls, *f* was calculated with a roughness of zero and multiplied by four (10). For the final design, a material roughness of 4×10^{-4} was high enough for this assumption to hold, and the containing walls where high convection was required were machined in such a way to produce grooves perpendicular to the flow, increasing the roughness of the walls in the axial direction. The trade-off to increasing surface roughness is that it also increases the head losses in the channel, which inhibit mass flow rate of water (10, 11).

Initial approximations of head loss in each channel were made on the chosen designs and indicated head losses would be less than 1psi for each cooling channel. This implies that the primary mode of head loss would come from sudden geometry changes, which are largely estimated with empirical approximations (11). Unable to find loss coefficients for all geometries used in the final design, keeping flow velocities low was

the primary design focus of the water delivery systems into each water jacket. For the purposes of design, each cooling jacket was assumed to have a water volumetric flow rate of 25% of the unimpeded flow rate from the supply used for this research. Since the unimpeded flow rate was measured to be roughly four gallons per second, each channel assumed one gallon per second of water flow.

The other goal of the water jacket designs was to prevent the metal in direct contact with the detonation channel from reaching high enough temperatures to soften or ablate. The temperature rise from the water side to the detonation side was modeled using Fourier's law for a cylindrical wall (Eq. 9), which gives the temperature difference between the inner and outer surfaces of a cylindrical wall due to a constant heat flux on the inner surface (10).

$$q = \frac{2\pi H \cdot k_W (T_{SC} - T_{SW})}{\ln\left(\frac{D_{SW}}{D_{SC}}\right)} \tag{9}$$

Based on the equation, if one of the diameters is fixed, three variables are involved in designing the walls. Highly conductive materials like aluminum and copper have a high *k* and will have a lower temperature rise for a given heat flux. At the same time, materials with high melting points permit a larger temperature change. Unfortunately, highly conductive materials typically have low maximum operating temperatures, while traditional high-temperature materials used in turbomachinery like Inconel have poor conductivity. One advantage the latter category has over the former is

that the latter works as an insulator, absorbing less heat from the detonation channel and requiring less intense cooling.

The third variable is wall thickness. Eq. 9 indicates thinner walls are best, so the wall thickness was designed to be the minimum thickness to withstand the high pressure of the passing detonation and shock waves. Since the pressure profile in the detonation channel is as 3D and unsteady as the temperature profile, mechanical stress modeling needed to be significantly simplified without advanced finite element analysis. With that in mind the pressure in the channel was assumed to be a uniform 400 psi based on pressures seen in previous research (2). This overestimate provided enough to calculate maximum hoop stress in the containing walls σ_h based on the pressure P, the outer radius of the wall r_{sw}, and the wall thickness t according to Eq. 10 (12).

$$\sigma_h = \frac{P \cdot r_{sw}}{t} \tag{10}$$

Using this formula and assuming a factor of safety of 3 to account for softening at high temperatures, the minimum thickness and corresponding temperature rise for a wide range of materials were calculated. After investigating several different materials and taking into account their conductivity, strength at high temperature, cost, and machinability, 0.100” of mild steel was found to be an acceptable wall thickness. A thinner wall would have been possible, but machining tolerances indicated 0.100” would be safer. This was used for the center body, while a pre-existing 0.070” 304 stainless steel wall was used for the outer body. Similarly, the cooling channels were designed to be 0.100” wide to allow sufficient cooling. These dimensions could not be optimized

without more precise knowledge of the heat production in the detonation channel, but initial calculations indicated these thicknesses would work well with the estimated heat.

The heat exchanger design chosen routed water through the center of a bullet-shaped body and forced the water to flow down the sides. The exit holes transitioned from wide ellipses to circles in order to reduce the pressure loss and avoid non-uniform flow along the cooling walls. While the center body was designed to be one welded piece, the outer body was designed as three pieces bolted together to facilitate cleaning. The water entered a manifold near the aft end of the RDE from four one-inch supply lines then flowed into the cooling channel. It then flowed out at the base of the wall into another manifold with four one-inch drain lines. Fig. 6 shows a computer-rendered model of the initial RDE design color-coded to help differentiate separate parts.

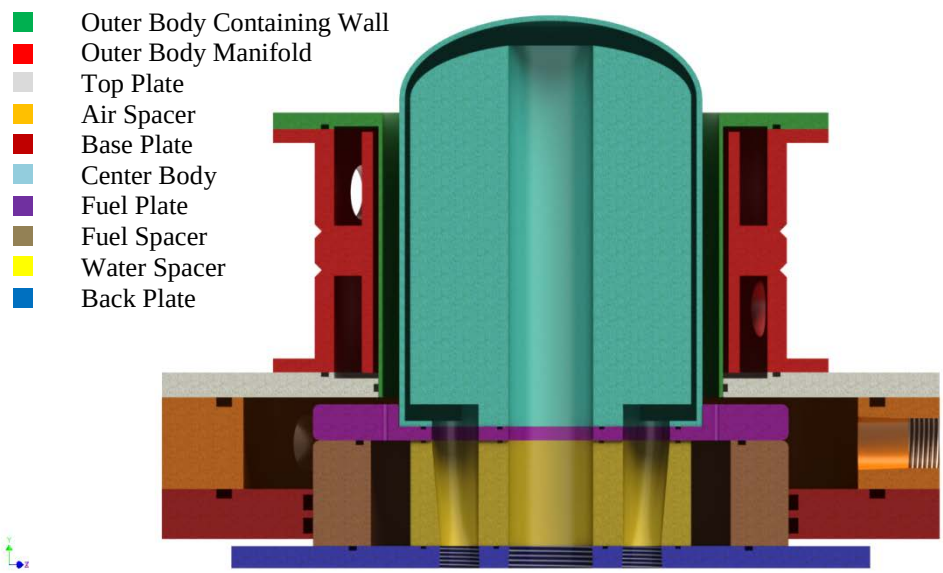

Figure 6. Original cooled RDE design cross-section model

One issue with these designs is the pre-detonator setup. Previous research RDEs use a low-mounted pre-detonator which fires directly into the detonation channel (2, 3). The advantage to this setup is that the detonation is initiated at the same height in the channel that it traverses during steady operation. Unfortunately, the water jacket designs used in the cooled RDE are incompatible with this type of pre-detonator. Specifically, the pre-detonator would not only interfere with even cooling flow along the outer body, it would require more complex machining and time to make than was available for this thesis. The solution was to mount the pre-detonator at the aft end of the RDE and fire into the channel.

Several mounting approaches were tested and their ability to propagate at least one detonation wave into the channel was recorded. Originally, the aft-end pre-detonator was modeled based on previous work, which assumed that the pre-detonator needed to be inserted at least partially into the channel (4). After much testing, it was found that the most consistent deflagration to detonation transitions occurred when the end of the pre-detonator was completely outside the channel. This can be attributed to the higher center body wall in the cooled RDE than in previous research, which provides a reflecting wall for the detonation wave to recouple against. Since the research cited in (4) had a lower center body, the pre-detonator was also angled slightly more toward taller outer wall, which could have served to reflect the detonation wave better. The final pre-detonator design was fixed to the aft face of the RDE and fired perpendicular to the detonation channel.

3.2 Deviations from the Design

During testing several problems forced changes to the original cooled RDE design. The first was failure of the gland seal on the outer body wall which was designed to stop the water from leaking into the base of the detonation channel. The first solution was to replace the hard FEP-encapsulated O-ring with a softer silicone O-ring. FEP works better with water than silicone but the softness of the silicone helps it to seal better. When that failed, the surface was polished to provide a smoother surface to seal against. That was enough to hold the seal until the RDE successfully detonated for two seconds.

The leak following that run was much larger than prior leaks. Inspection of the inner wall showed that not only had the high-temperature silicone O-ring partially melted, discoloration of the stainless steel at the seal indicated it had reached very high temperatures similar to those seen on the detonation side of the cooled wall. The stainless steel wall had also become pinched at the end, increasing the gap beyond the O-ring's ability to seal the water in (Fig. 7). It was believed that at the seal, the uncooled extension of the wall had annealed under the high temperatures and pressures of the detonation waves and had contracted when cooled by the air and water after the two-second run had finished.

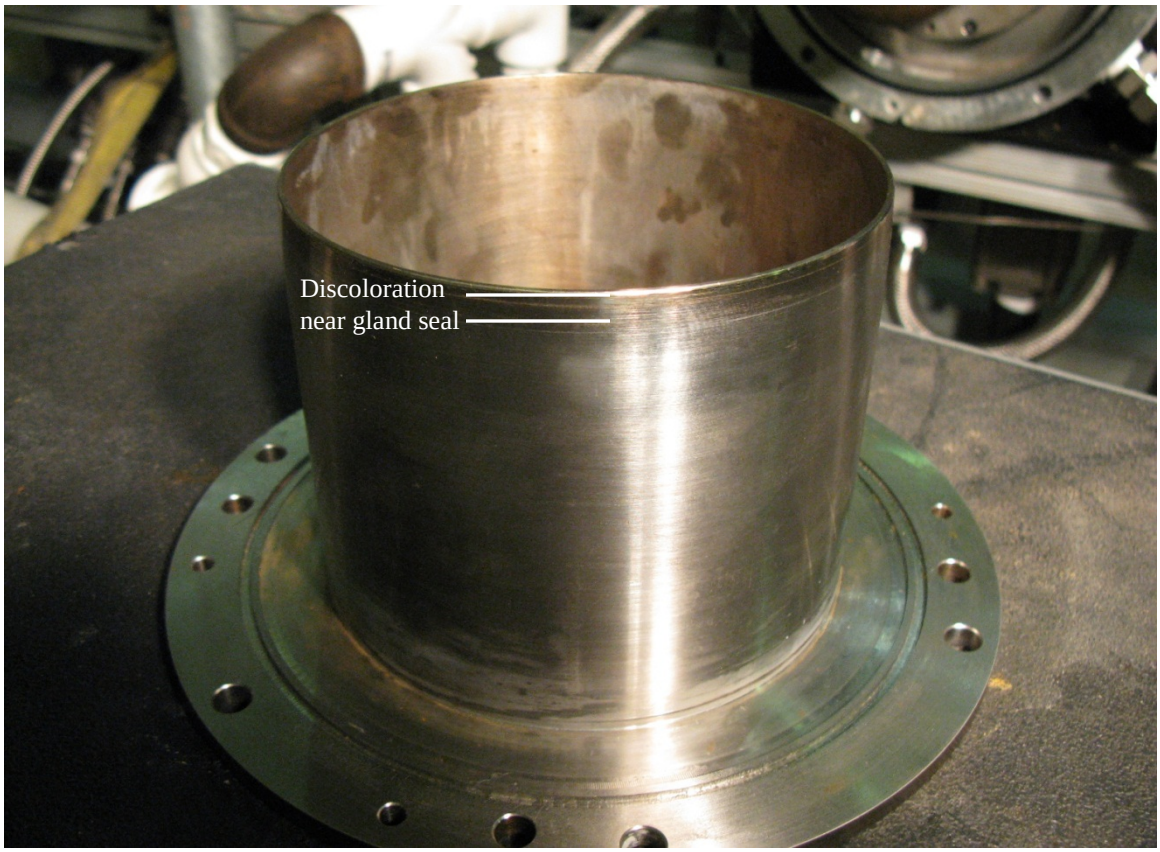

Figure 7. Stainless steel outer body containing wall after two-second operation

The two solutions available were to either replace the wall with a more conductive material, hoping that hot gasses were not entering the gland seal to melt the O-ring directly, or to cut a deeper channel into the top plate to allow better cooling at the base of the detonation channel and weld the seam shut. The latter was chosen for both time concerns as well as doubt that the designed gland seal would still work even with a more conductive material. The thermal expansion expected in the wall was accounted for by placing a neoprene gasket between the aft flange and the water manifold. The outer body was welded with the gasket compressed by 50%. After welding, the bolts at the flange were loosened to allow the expected 0.040” of expansion.

3.3 Cooled RDE Experimental Setup

The cooled RDE was tested on the RDE table in the Detonation Engine Research Facility (DERF). This table provided mounting framework, instrumentation ports, hydrogen fuel, air, and oxygen and hydrogen pre-detonator lines. The RDE was mounted horizontally on the so that steady-state exhaust products would flow into the exhaust bay and out of the testing cell (Fig. 8 and Fig. 9).

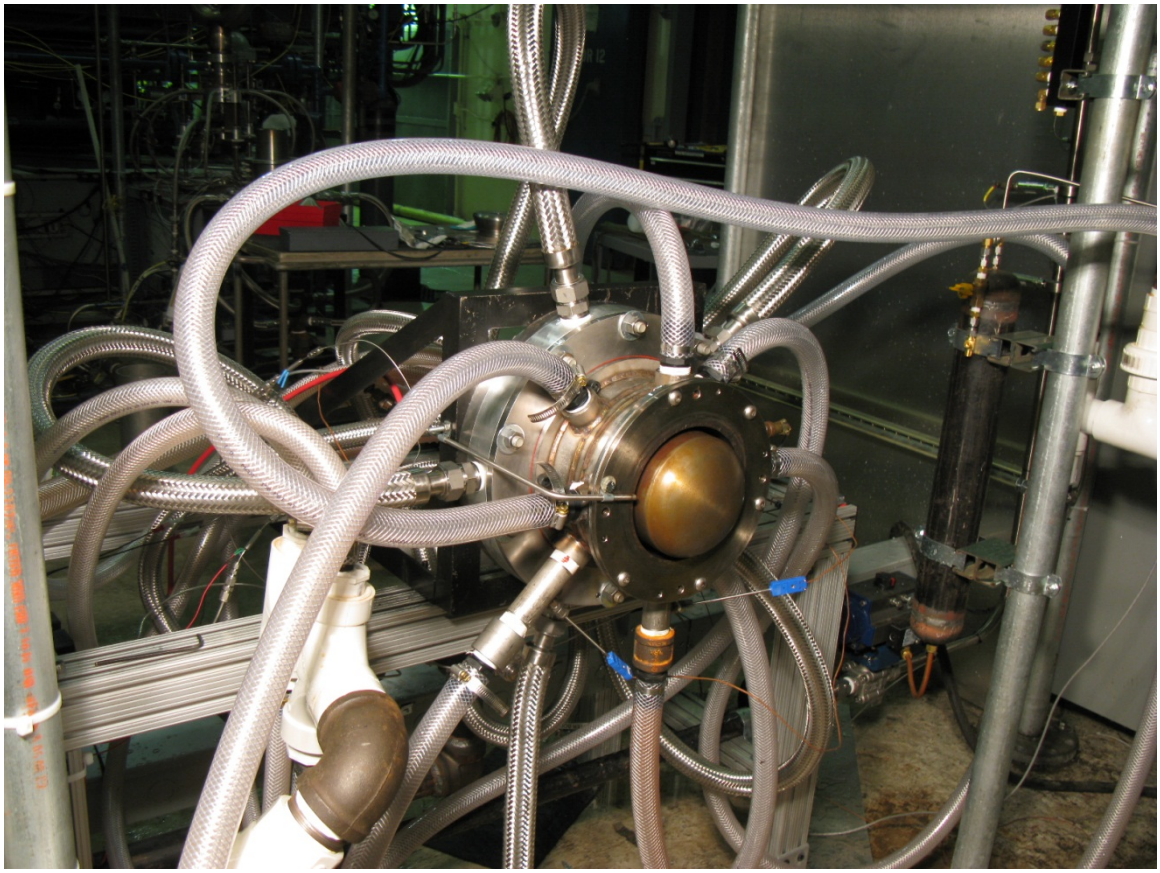

Figure 8. Aft end of fully assembled water-cooled RDE after all modifications

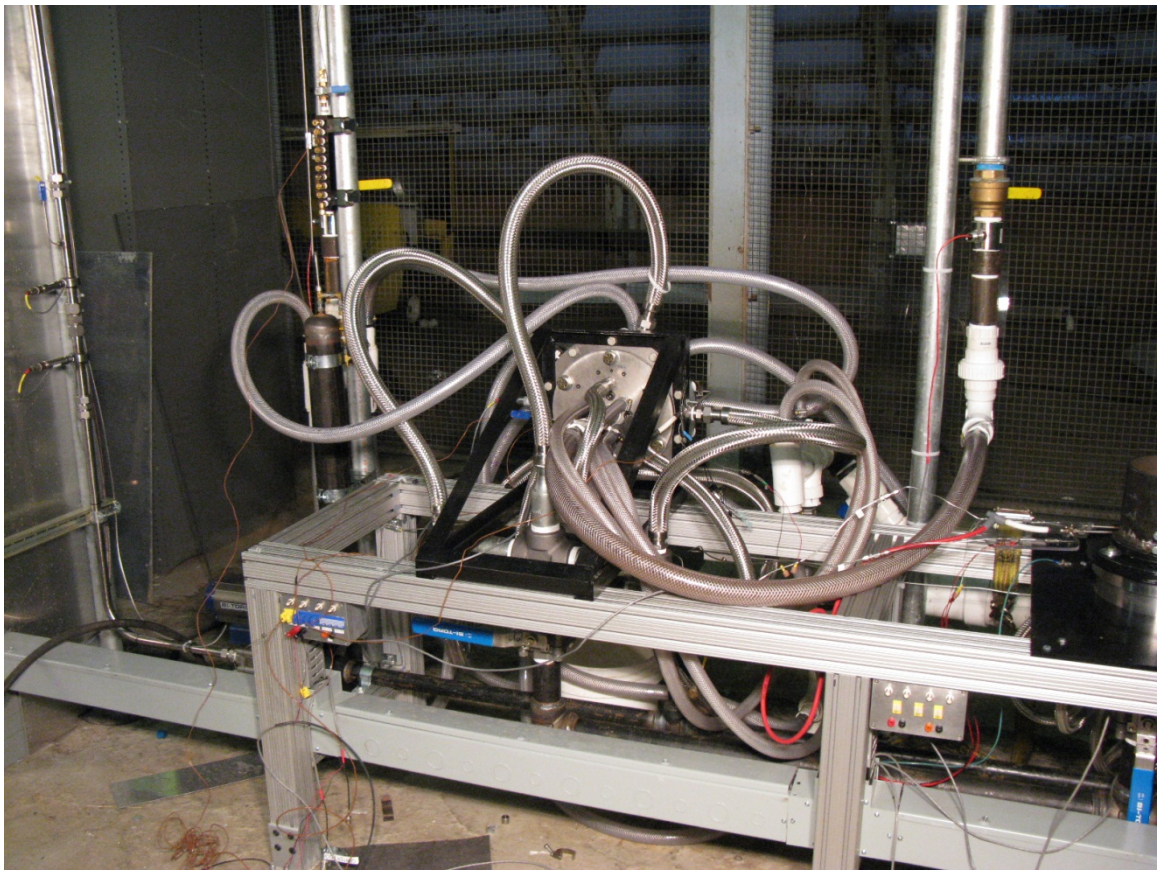

Figure 9. Fore end of fully assembled water-cooled RDE

Air was supplied to the RDE table from a storage tank outside the test cell. The first components in the line after air left the tank were several manually activated pneumatic safety valves, which prevented air from entering the lines before a test. These valves, also present on the fuel lines, were also used to cut the fuel and air supply during a long run if it needed to be aborted. The desired flow rate was adjusted by requesting a static pressure in the line from the control program, which would communicate with a pressure regulator to determine the size of the orifice the air would be allowed through. Further downstream were manual ball valves which were opened or closed to allow air to the RDE table and not elsewhere in the test cell. Following these was a critical nozzle

with a precise diameter which would choke flow and ensure mass flow in the supply lines could be determined using static pressure data. Pressure and temperature sensors upstream and downstream of this nozzle enabled mass flow rate derivation. Immediately following the critical nozzle was a pneumatic valve which the control program opened at the start of the run and closed after the establishing time and operating time had passed. Finally, manual ball valves under the RDE table determined which RDE would receive air flow.

The hydrogen was supplied in a similar fashion, also starting outside but from a trailer of hydrogen tubers rather than a fixed tank like the air supply. The only other difference was that before reaching the regulator, the line branched off to supply hydrogen to the pre-detonator setup. After this branch, the hydrogen going to the pre-detonator went through a manually activated ball valve to allow or disallow it to the pre-detonator. Next was a pressure regulator fixed to allow 200 psi to the pre-detonator. Next were two three-way valves used to send the hydrogen to pre-detonator setups elsewhere in the bay. The last component in the pre-detonator line was a fuel injector, which could be modified for different pulse widths on the order of 20ms. The oxygen for the pre-detonator was supplied by bottle inside the test cell and fed the pre-detonator line in the same way as the hydrogen pre-detonator line.

Water was provided from two pipes connected directly to the city main line. One pipe delivered water to the outer body, and one delivered water to the center body. Each used a turbine flow meter to measure water mass flow through the RDE. T-type thermocouples measured water temperature entering and leaving the RDE through the outer body and center body. A view of the thermocouple used to measure the

temperature of water entering the center body through the 1½” hose is presented in Fig. 10. Water leaving the RDE was routed through the exhaust bay and drained outside. Two ball valves placed in the lines before they join at the outlet enabled imprecise throttling of the flow rates.

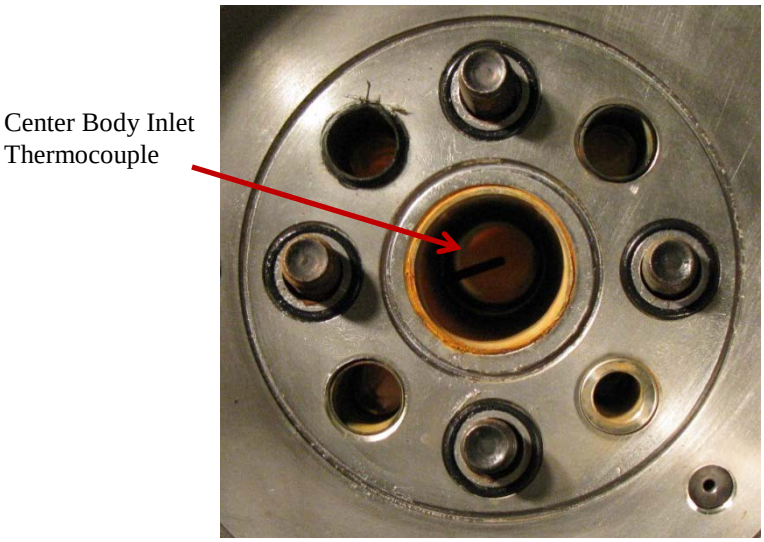

Figure 10. Cooling water ports for the RDE center body with thermocouple visible

Since the complex geometry of the water jackets and high heat into the walls prohibited the use of PCB® dynamic pressure transducers normally used in the DERF to record wave speed, detonation velocity was recorded using high-speed video of the detonation channel (2, 3). By recording at a frame rate of 40000 fps and an exposure time of 24μs, detonation waves could be tracked. The detonation velocity was calculated by counting the number of laps completed by a wave during steady operation, dividing by the number of frames, multiplying by the frame rate, and multiplying by the detonation channel outer circumference.

The high-speed video was also instrumental in finding the operational space of the cooled RDE. Since the pre-detonator was a new design, failure to detonate a given mixture was either due to poor pre-detonator design or a bad mixture. On the high-speed video, it was found that sometimes the flash at the end of the pre-detonator would end abruptly without forming the typical two-wave pattern seen in 6-inch RDE detonations. This indicated either a bad pre-detonator or a mixture far outside the operational space. If, however, there was no flash at the exit plane of the pre-detonator and the typical two-wave pattern started within the channel, but no stable detonation was established, the pre-detonator was considered to be functioning but the mixture was outside the operational space. The high-speed video also indicated poor mixing in the fuel manifold by showing that detonation waves were brightest when passing over the four fuel lines. This helped to establish the need for higher equivalence ratios and high flow rates to compensate (3). Although this unsteadiness diminished quickly, the fuel and air supply program was only designed to provide constant flow rates throughout the run, so manually changing flow rates after startup was not possible.

3.4 Cooled RDE Testing Procedure

Before running the RDE to steady temperatures, several checkpoints had to be met. Since data collected was not printed to the control program until after each run, operating time was increased slowly, starting at the half-second time typically run on uncooled RDEs. These runs were used to identify stable operating points for the RDE to ensure the engine could detonate consistently and predictably. This was often difficult, since mass flow rates for both hydrogen and air were controlled by requesting a pressure upstream of the critical nozzle for each supply line. The program then opened an orifice

for each line to enough to reach the desired static pressure. At the RDE table this typically resulted in lower pressures than requested and one input pressure often corresponded to a range of measured pressures.

For each run, an air establishing time of 2.5 seconds was used along with a fuel establishing time of 1 second. Establishing time referred to the length of time air and fuel would be blown through the RDE before the trigger was sent to the pre-detonator to ignite. These were used to minimize unsteadiness in the flow immediately preceding ignition. Operating time or run time was controlled by the fuel operating time. Runs ended when fuel was cut, while air flowed for another second to purge the engine of fuel.

After each run, the pressure upstream of the critical nozzles in the air and fuel supply lines at the 2500ms mark were recorded and used to calculate mass flow rates and equivalence ratio at startup. Whether or not the mixture detonated was also recorded, as was any unusual behavior which could affect the run. Successfully detonating runs in this RDE were observed in four ways: high-speed video, low-speed video, sound, and manifold pressure. On the high-speed video, detonations could be visibly traced, and wave speed during steady operation could be calculated. This was the primary way of indicating a successfully detonating run. A successfully detonating mixture also showed an increase in both fuel and air manifold pressures in the RDE, while a deflagrating mixture showed no increase. Although this is a sign of pressure gain combustion, it does not provide enough information to prove that a mixture detonated and only served as initial confirmation.

Qualitative observations accompanied detonations and were accurate indicators, but were not relied on as definitive. Since these observations could be made during the

run, they were used to determine if a run needed to be aborted due to a bad start before wasting large amounts of hydrogen. Visually, on the low-speed cameras in the control room, the plume from a detonating run appeared as a short, sharp, less intense flame (Fig. 11), while a deflagrating flame appeared as a longer, wider, and brighter flame (Fig. 12). Detonating runs were also accompanied by a loud, intense roar, while deflagrating mixtures were accompanied by a shriek. This contrasts with the sound made by other RDEs, which get louder and shriek during detonating runs (2, 3). The shriek has been attributed to the frequency of the rotating detonation inside the engine, so its presence in a deflagrating flame implies an interesting unsteadiness in non-detonating flames.

Figure 11. Low-speed capture of detonation in the cooled RDE

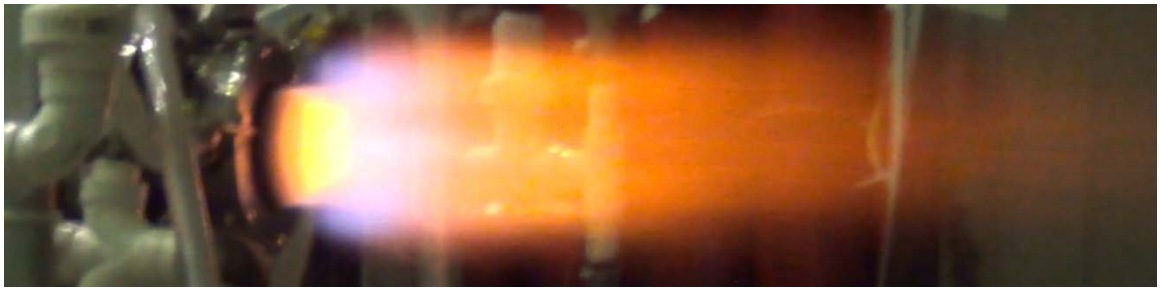

Figure 12. Low-speed capture of deflagration from the cooled RDE

These initial half-second runs were done with water in both the outer body and center body but not allowed to flow. With a combined flow rate of 2.9 gallons per second emptying outside the test cell, water was only flowed when ready to push for longer operating times. Run times increased from 0.5 seconds to 1, 2, 5, 10, and 20 seconds. For all runs longer than 2 seconds, the three primary concerns were mechanical failure of the RDE due to metal overheating, failure of the water lines due to water overheating, and the danger of exhaust products re-entering the test cell. A thermocouple placed above the engine exhaust plume was used to ensure hot gases were not recirculating into the bay while an infrared thermometer measured the temperature of the ceiling of the test cell. Both temperatures were read continuously from digital displays to allow mid-test emergency shutdown. Several cameras were aimed at the RDE setup to allow visual inspection of the engine and supply lines during testing. However, the best indicator of overheating was the water jacket exit thermocouples, which could show both the water temperature important to safety in the water lines and total heat rate, which in turn could be used to estimate wall temperature in the detonation channel. Since these were only displayed at the end of each run, these were the primary drivers in the decision to gradually increase operating time to the 20 second run.

3.5 Heat Flux Gauge in the Uncooled RDE

The gauge used to measure transient heat flux in the RDE was designed by Turbine Research Facility for use in PDE and RDE research. The gauge functions as a four-wire RTD, using high-temperature materials to survive in detonation environments. The platinum in this gauge is roughly 100 angstroms thick and was deposited on a ceramic substrate to form the desired circuit shape. The substrate was in turn attached to

a Hastelloy rod, which provided structural support for the gauge. Current was sent through the outer two leads to the platinum on the face of the gauge, while the inner two leads measured the voltage across the face. The heat flux gauge is shown in Fig. 13 and Fig. 14.

Figure 13. Sensing face of the heat flux gauge

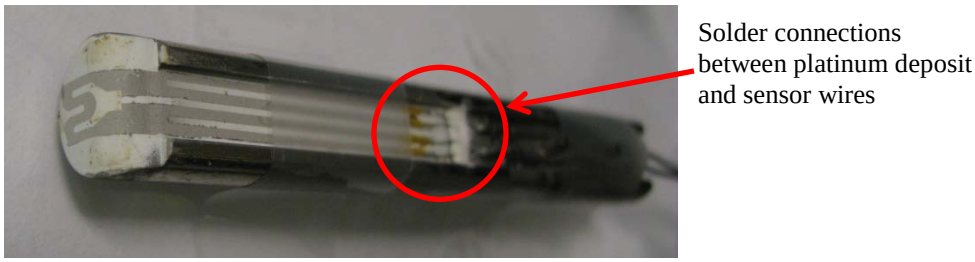

Figure 14. Heat flux gauge with protective cover and potting material removed

Ceramic potting material filled in the fillet on the face of the gauge to maintain a flat surface, but in experiments this material was usually blasted out of the gauge in the first run. This often caused the gauge to leak gasses from the detonation channel through the back of the gauge, weakening the solder points and likely contributing to their failure. The probe used to collect the data for this research replaced the blown-out potting ceramic with JB Weld®, a tough metal epoxy. While this was also blown out by the detonation waves, it was slightly more resilient than the ceramic.

The heat flux gauge used in this experiment was calibrated in a silicone oil bath from 70°F to 230°F and was found to have a thermal resistivity coefficient of 0.00201 [1/°K]. The linearity of the resistance over that temperature range is shown in Fig. 15. A similar gauge was calibrated over a wider range, but it was found that soaking the entire length of the probe at high temperatures destroyed the sensitive solder connections between the platinum deposit and the electrical leads, visible as the orange portion of the gauge in Fig. 14.

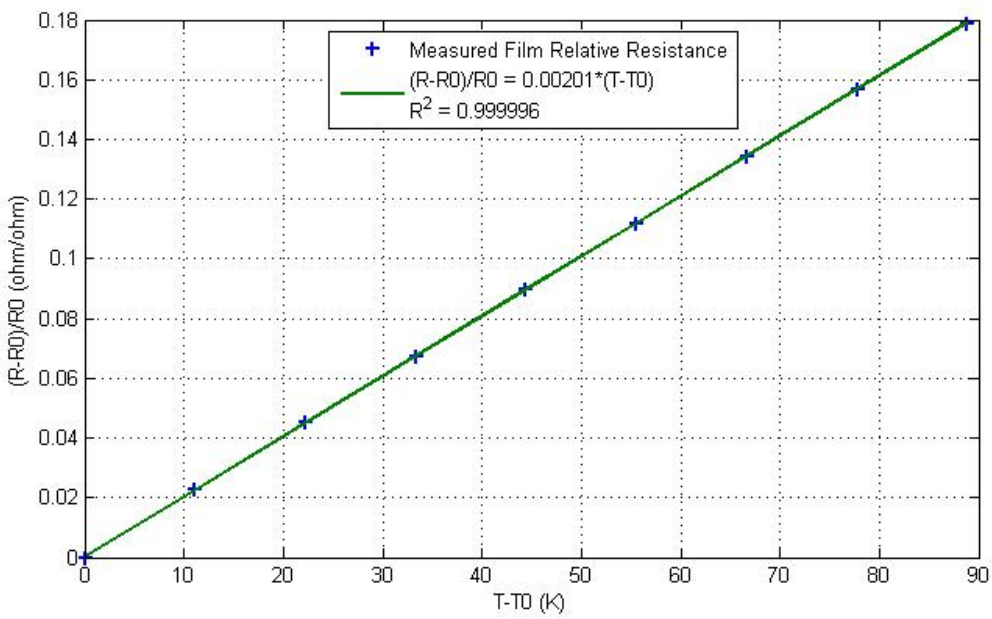

Figure 15. Heat flux gauge non-dimensionalized resistance vs. temperature

In order to maintain constant current to the gauge, it was connected in series to a 10 kΩ resistor and a 0.1 ampere power supply. The resistor helped the power supply to remain nearly constant despite variations in the much lower resistance of the gauge. This circuit was first tested using an off-the-shelf 4-wire ceramic-insulated RTD. This RTD

showed only 138°C rise in the wall temperature after 600ms and no unsteadiness in the rise, confirming the need for a more sophisticated gauge with a much faster response time.

3.6 Uncooled RDE Test Setup

This heat flux gauge was tested on the 6-inch RDE in the DERF (2). The normal 6-inch RDE outer body was replaced with one designed for five ports spaced at 1" intervals to allow for axial instrumentation using the custom RTD. The resulting outer body was 0.5 inches taller and had five half-inch Swagelok compression fittings in place of one of the instrumentation port columns. The center body used was also taller than that used in previous research to better compare with that of the water-cooled RDE. This setup is shown in Fig. 16.

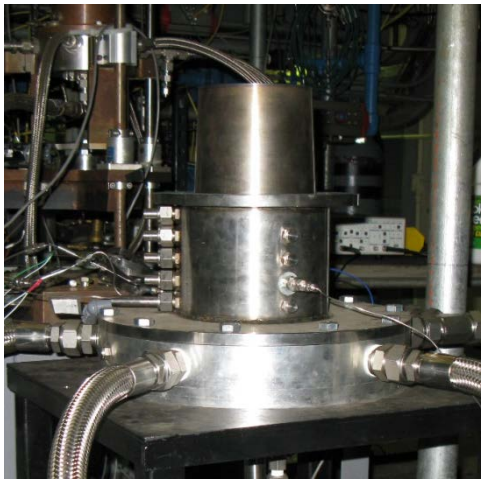

Figure 16. Modified 6-inch RDE used for heat flux gauge testing

A PCB probe was located 3.375" from the base of the detonation channel and was spaced 120° clockwise from the heat flux gauge. The heat flux gauge was tested in the

lowest position, with the center of the face 1.125” from the base of the detonation channel. The gauge was oriented with the filled-in radius aft of the platinum sensor to minimize its effect on the measured flow. Both the PCB and heat flux gauge data were collected unfiltered by the high-speed data card at a sampling rate of 1 MHz.

CHAPTER 4. RESULTS AND DISCUSSION

4.1 Cooled RDE Operating Point

While the operational space for this RDE was not fully mapped, an operating point where the RDE could be relied on to successfully detonate was found. This point was around a total mass flow rate of 220 lb/min and an equivalence ratio of 1.11. Both the total flow rate and the equivalence ratio are greater than the starting operating point used for the uncooled 6-inch RDE of 175 lb/min and 1.0, respectively (2). This indicates worse mixing between the air and hydrogen. Since the only difference in the gas flow paths between the cooled and uncooled RDEs is the fuel manifold, it is believed to be the cause of the high required flow rate. Increases in detonation wave brightness on high-speed video which corresponded to the locations of the fuel inlets also contributed to this belief. A steel plate was welded into the fuel manifold in an attempt to distribute the jets caused by the four fuel inlets more evenly, and detonation waves observed on high-speed video were no longer brightest over the fuel inlets. However, high mass flow rates were still required for successful initiation.

4.2 Steady-State Heat Rate

The water-cooled RDE was run for up to 20 seconds. Longer runs could be tested, but the current testing configuration indicated significant recirculation of the exhaust products back into the test cell, endangering the surrounding equipment. Mixing air blown from behind the engine helped to keep hot air from re-entering the test cell, but

a shield over the engine will likely be required to keep the surroundings cool during longer tests.

The RDE itself appeared to reach near thermal equilibrium very quickly, reaching the steady-state average within the first two seconds. The noise in the thermocouple signals inhibited calculation of heat rate into each wall as a function of time, but average signal from each thermocouple was steady enough to use to calculate heat rates. Of the four runs, the one with the steadiest hydrogen supply maintained a constant mixture composition for 10 seconds, so the average heat rate of that run was calculated between 5 and 10 seconds after ignition. Each heat rate was calculated according to Eq. 2. For a mixture with a total mass flow rate of 220 lb/min and an equivalence ratio of 1.08, the heat absorbed by the outer body was 141 kW and the heat absorbed by the center body was 409 kW. The difference in heat rate can be explained by the several differences between the two walls.

The most prominent difference is that the center body is made of mild steel, which has a much higher conductivity than the stainless steel used in the outer body. This means that more heat is required to maintain a high detonation channel wall temperature. Since all forms of heat transfer are some function of the difference in temperature, and the temperature in the channel should not change significantly between the inner and outer walls, the heat rate to the center body should be greater than the heat rate to the outer body. Additionally, the dome at the aft end of the center body accounts for about 35% of its exposed surface area. While the convection on this surface is lower than inside the detonation channel due to much lower flow velocity, radiation from the plume may be significant.

The difference in heat transfer due to conductivity of the wall can be accounted for by the ratio of each wall's thermal resistance, k_w/t (10). The outer body wall's thermal resistance is a little under double that of the center body. Including the slight difference in surface area exposed to the detonation channel, and the heat flux into the center body in the detonation channel should have been only 4.4 MW/m^2. Moreover, this approximation assumes the same temperature rise over each wall, which would not be supported under higher heat rates. At thermal equilibrium, the heat rate from convection and radiation into the wall must be equal to the conductive heat rate through the wall. Both convection and radiation are functions of the wall temperature, so the wall must be cooler to support higher heat transfer rates. Thus, the heat transfer rate into the center body from the detonation channel must be less than 4.4 MW/m^2. This leaves over 100 kW of heat that cannot be accounted for from the detonation channel, implying the dome under the exhaust plume averaged over 6.4 MW/m^2. Further research must be done to examine the heat transfer specifically in this region.

It is important to note that increasing the hydrogen flow rate increases the HHV of the mixture. While the RDE was designed assuming a hydrogen mass flow rate of 5 lb/min, the steadiest run had a hydrogen mass flow rate of 6.7 lb/min. This resulted in an increase in HHV to 7.16MW, meaning the outer body and center body water jackets extracted 2.1% and 6.1% of the HHV as heat, respectively. Both of these ratios are lower than that seen in the 3-inch RDE, but that may be due to a poor estimation of total enthalpy. If the total expected enthalpy is assumed to be the lower heating value (LHV), which assumes all water products remain gaseous, the outer body and center body extract 2.5% and 7.1%, respectively. LHV is also a more realistic estimation of the total

enthalpy rise, since the high temperatures in the exhaust make condensation highly unlikely. The percentages associated with the LHV match the center bodies between the two RDEs, but still indicate lower heat extraction to the 6-inch outer body wall than into the 3-inch outer body wall. As mentioned above, this is likely because the stainless steel used in the 6-inch outer body is a better insulator than the mild steel used in the cooled 3-inch outer body. The lower height of the outer body wall may also play a factor, since increased channel height means more of the plume stays inside the annulus.

4.3 Design Lessons Learned

The largest assumption made during design was that the outer body wall near the base of the detonation channel could survive without water cooling. The high contact resistance between the wall and the 0.341” top plate, the low surface area exposed to fresh air, and the high net heat flux from the detonation waves caused an almost catastrophic failure (Fig. 17). While the first two contributors were expected to some extent, it was believed that the fresh air entering the channel behind each detonation wave would contribute to cooling (5). While this may have occurred, unsteady detonation behavior in the RDE likely decreased the refill height and consequently the surface area of the wall cooled between detonation waves.

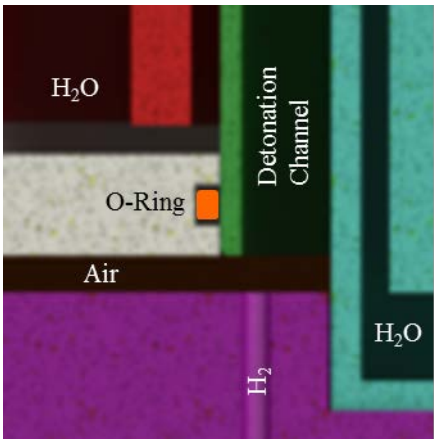

Figure 17. Failed gland seal design for outer body wall

The second poor assumption made led to the decision to only use four fuel lines to inject fuel into the RDE. The assumption was that in order to maintain low flow velocities in the manifold and reduce the speed of the jets leaving the inlets, the total inlet area should be the same or more on the cooled RDE as on the 6-inch RDE. While this was satisfied, bringing total area from .55 in^2 to .69 in^2, no consideration was made for the fact that the designed inlets in the cooled RDE faced directly into the holes in the fuel plate, while the 6-inch RDE fuel inlet jet stagnated against a flat plate centered in the RDE. There was more than enough room on the back plate to add ½NPT fittings for eight fuel lines, but only four were used to reduce cost. Eight jets would greatly improve consistent fuel flow rate around the channel by reducing the jet velocity for each inlet and reducing the distance between each jet. Another solution to improving mixing would be adding a second plate in the fuel manifold to force the jet to stagnate against something earlier in the manifold.

4.4 Low Equivalence Ratio Runs in the Cooled RDE

While all runs attempted to use the same mass flow rates of both air and hydrogen, the hydrogen supply tended to lose pressure during a run. This meant that during some runs the mass flow rate of the hydrogen dropped significantly while the mass flow rate of air remained constant. This phenomenon was observed in short runs, but the operating time was too short to notice what, if any, effect it has on RDE operation. Then, during a two-second run, the hydrogen pressure upstream of the nozzle dropped from 480 psig to 170 psig, indicating an equivalence ratio drop from 0.97 to 0.4 (Fig. 18).

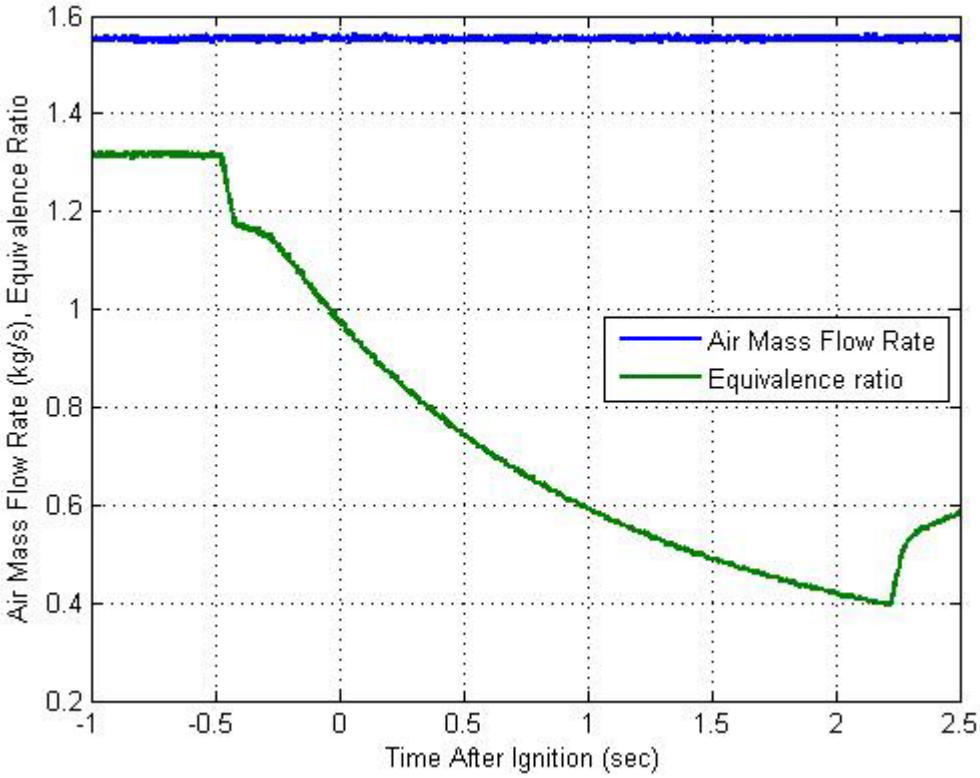

Figure 18. Air mass flow rate and equivalence ratio over time during a 2s run

Moreover, the low-speed camera showed the plume shrink from roughly three feet to only one foot (Fig. 19). Both the air and fuel manifold pressures indicated a small decrease while the engine continued to make the loud, sharp roar associated with detonation. Finally, faintly visible detonation waves were still present in the channel a full 1.5 seconds after ignition. This was in contrast to longer runs where the detonation wave brightness was washed out by the plume brightness within the first 100ms. While other long runs also saw drops in equivalence ratio, this run experienced the most dramatic change and implies that once an RDE starts it can maintain the detonation wave for a much wider range of equivalence ratios.

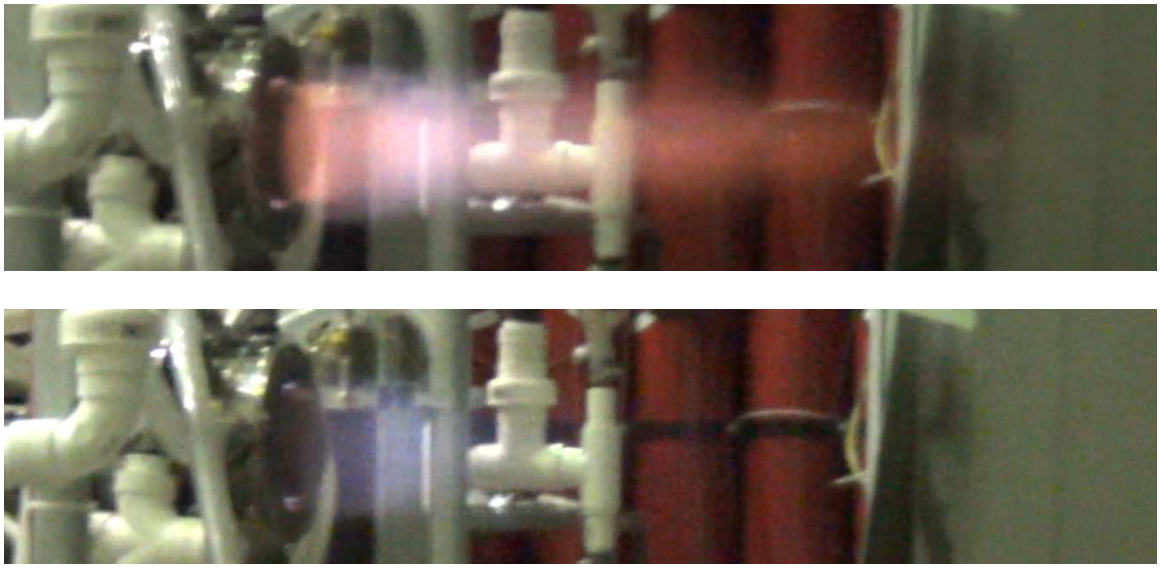

Figure 19. Comparison of detonation exhaust plumes at equivalence ratios of 1.05 (top) and 0.84 (bottom)

4.5 Heat Flux Gauge Results

The heat flux gauge only successfully recorded a low noise signal once, during a test of a mixture with a total mass flow rate of 223 lb/min and an equivalence ratio of 1.07. The gauge in this test recorded data for 43ms before a strip of platinum and the ceramic substrate below separated from the face of the gauge. A comparison of the face of the gauge before and after the 500ms test is shown in Fig. 20. While this had occurred on another gauge tested in the RDE, the other gauge broke after several detonating runs, while this gauge broke on its second detonating run. Since the failed ceramic was under JB Weld® at the start of the run, it is possible the epoxy pulled the substrate with it as it was worn down in the detonation channel.

Figure 20. Heat flux gauge before and after data collection

Despite the mechanical failure of the probe, the data gleaned in the first 43 milliseconds was exceptionally clean. As shown in Fig. 21, the gauge indicated a 300°C

rise in wall temperature before the gauge broke. This is in stark contrast to the 138°C rise in 500ms seen from the off-the-shelf RTD.

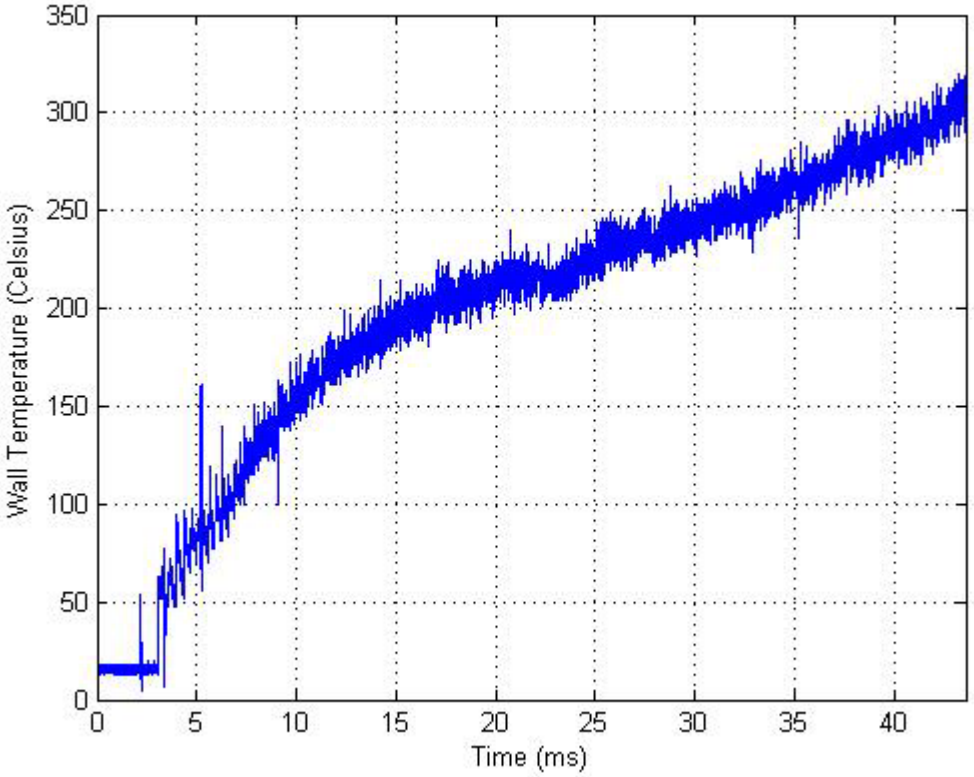

Figure 21. Wall temperature in the first 43ms of RDE operation

In addition to the overall rise seen in this period, the gauge also showed very detailed and clean temperature waveforms during startup. Fig. 22 shows the heat flux into the gauge, temperature on the face of the gauge, and the pressure in the channel detected by the PCB immediately following ignition. The sharp spikes seen around 3.3ms, 5.2ms, and 5.3ms are most likely electronic noise, as these were also present on low-frequency pressure data taken in the same run.

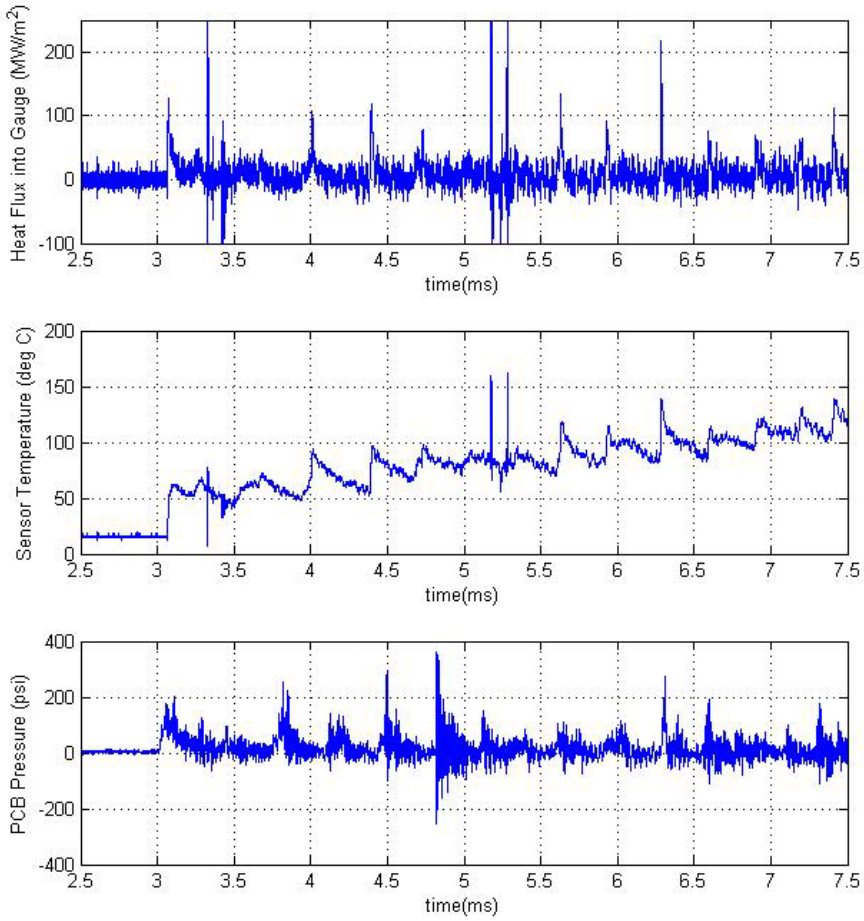

Figure 22. Heat flux, temperature, and PCB pressure during startup

When the temperature is transformed into heat flux, the step change corresponding to the passing detonation waves becomes much more pronounced. At the same time, the digitization-level noise from the temperature trace becomes much stronger. This is because the heat flux is highly sensitive to the time derivative of temperature, which greatly amplifies even low noise. During startup the temperature waveforms are each reflected by the calculated heat flux as high-heat impulses, while the heat flux corresponding to smoother temperature waves is largely lost in the digitization

noise. This startup period immediately following the pre-detonator provides the cleanest heat flux signal, while later intervals are too weak to easily observe heat waveforms.

For this run, steady wave behavior was elusive. Steady behavior is the best indication of detonation activity, since it makes finding wave speeds easiest. High enough wave speeds indicate detonation waves, around 1400-1600 m/s for hydrogen and air. Analysis of the PCB data indicated a wide range of detonation velocities, with the largest concentration around 3100 m/s (Fig. 23). Since only one PCB was used, this high speed indicates two-wave operation. Two-wave operation is characterized similarly to steady operation, but instead of one wave travelling around the annulus, two waves rotate around the channel in the same direction at the same speed as a single detonation wave. In this case the detonation velocity would be 1550 m/s. Two-wave operation has been seen in other RDEs but had not been observed in the 6-inch RDE before this test (2, 5). Since the heat flux gauge was tested at higher mass flow rates than had been tested before, it may be that two-wave operation is normal above a threshold flow rate. More experimentation at high flow rates is necessary to confirm that assumption.

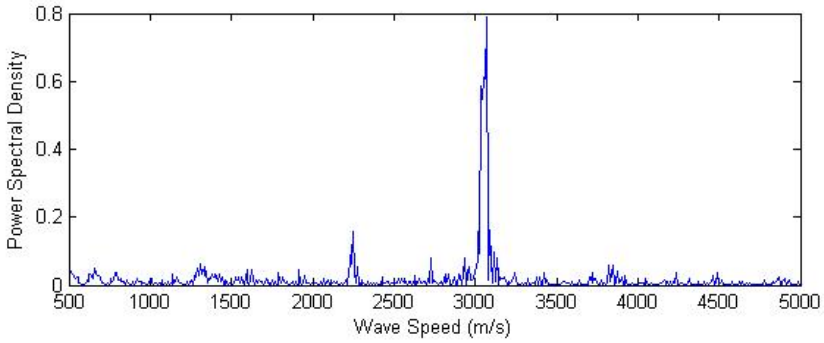

Figure 23. FFT distribution of wave velocities measured from PCB pressure rises

One characteristic of two-wave operation is lower detonation height. The refill period between each wave in two-wave operation is half the refill period for single-wave operation, so the height of each wave is lower. Since an oblique shock trails each detonation wave, the detonation height has little effect on PCB pressure. The heat flux gauge would be affected much more. Below the detonation height, the hot gasses in the detonation followed by cool reactants in the refill region make a simple temperature waveform for the heat flux gauge to sense. Above the detonation wave, there is no refill region to cool the gauge. Additionally, while the oblique shock increases temperature, the increase is much lower than that of the detonation wave, and it is followed by a shear layer where unsteadiness in the flow and deflagration of unreacted propellants make the temperature profile much more complex (4).

Around 40ms after ignition, the PCB began to record nearly constant wave speeds near 3000 m/s. If this were two-wave behavior, the lower detonation height could explain why the temperature waveforms are less obvious and why the heat flux signal is indistinguishable from noise during this period (Fig. 24). It is important to note that the range of heat flux during this period is within 50 MW/m^2, while during startup it was within 20 MW/m^2. This could indicate real, but very complex waveforms, or simply greater noise.

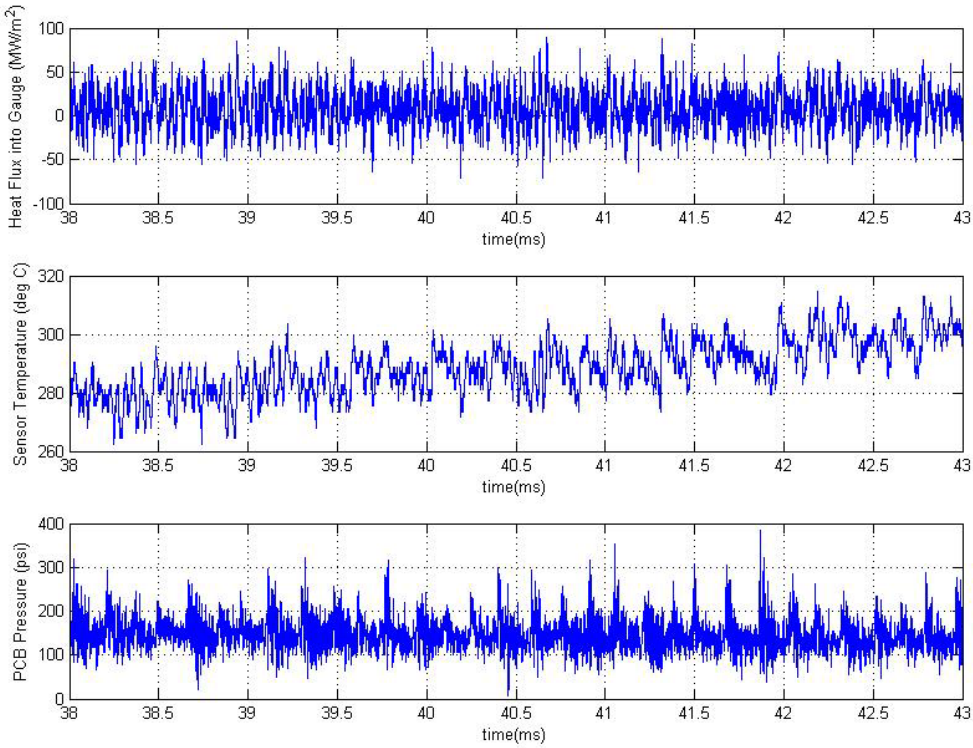

Figure 24. Heat flux, temperature, and PCB pressure after 38 ms

While two-wave operation is a reasonable explanation of the PCB pressure, it is also possible that there was no steady operation during the run, like the water-cooled 6-inch RDE, and that even spacing between pressure waves was coincidental. If this were the case, detonation height, wave speeds, and temperature profiles would vary greatly. Unsteady operation is a common occurrence in RDEs with periods of steady behavior, so the average heat transfer would still be useful.

While noise obscures most of the heat flux waveforms, the average heat rate was non-zero. Fig. 25 shows a backward-looking moving average of the heat flux during the first 43 ms using a two-millisecond averaging interval. Two milliseconds represents roughly six wave passes during single-wave steady operation (2), so this interval length

minimized the effect on varying wave speeds without losing the progression of the average heat flux. While the instantaneous heat flux into the gauge were on the order of 100 MW/m^2, the average heat flux varied around 8 MW/m^2. Had the gauge lasted longer, one would expect to see the average heat flux gradually decrease as the wall heated.

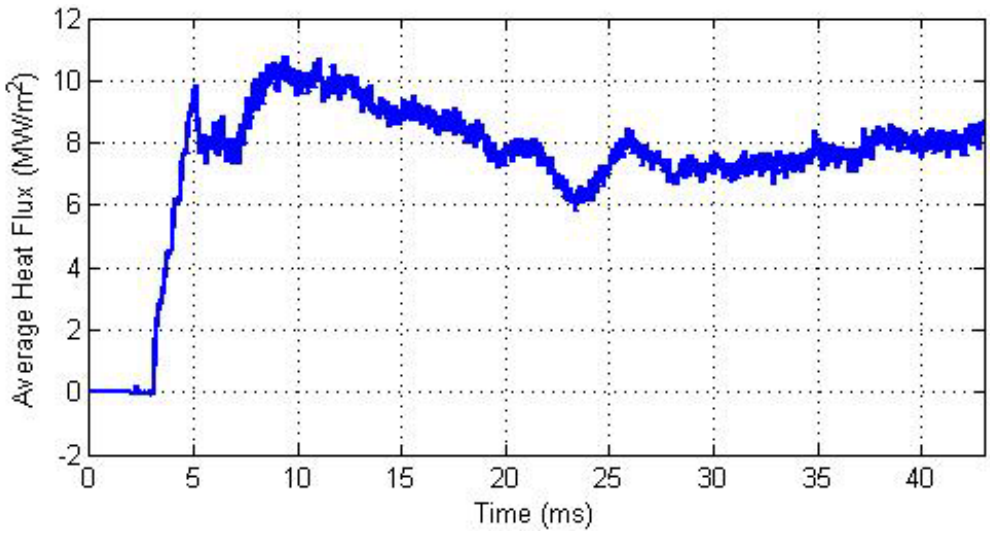

Figure 25. Average heat flux into the gauge

4.6 Comparison

The average heat flux measured from the heat flux gauge represents the heat flux into an uncooled outer body at one axial location. It indicated that at that position, average heat flux at thermal equilibrium should be no greater than 10 MW/m^2, since the heat rate into the wall should decrease as the wall's temperature rises. Meanwhile, the heat rate into the water-cooled RDE under very similar flow rates was 141 kW. Assuming constant heat flux, the steady-state heat flux into the cooled RDE would be 2.2 MW/m^2.

There are several reasons why the average heat flux into the cooled RDE would be lower than that measured by the heat flux gauge. The first reason is that heat flux gauge only operated for 40ms. In this time, the gauge temperature increased rapidly to over 300°C, and Eq. 9 indicates that for the cooled RDE outer body, even 2.2 MW/m^2 would yield a wall temperature of 290°C. That means the lower temperatures seen by the gauge during most of its operating time would draw more heat out of the detonation channel than the cooled walls would at thermal equilibrium, but once the surface of the gauge reached the same temperatures seen in water-cooled RDE, the heat flux should have gone down to 2.2 MW/m^2.

The heat flux gauge would only have reached that lower average if the assumption of constant heat flux over the entire outer body wall were correct. More likely, the average heat flux is greatest near the detonation activity at the bottom of the channel and decreases axially through the channel as temperatures drop and less energy is produced by combustion events. This has been seen using low response time instrumentation, with the average heat rate greatest at the top of the detonation wave, lower near the base of the channel and lowest in the region aft of the detonation activity (13). This gauge or similar devices should measure heat flux in the RDE at different locations to compare the axial distribution of the heat flux to the outer body wall.

The significance of these two sources of heat flux is that this is a large amount of heat, much more than the 200 kW/m^2 seen in PDEs at steady state (1). It stands to reason that under this intense heat, actively cooling RDEs is necessary to operate for long periods of time.

CHAPTER 5. CONCLUSIONS AND RECOMMENDATIONS

5.1 Conclusions

While the operational space of the water-cooled 6-inch RDE seemed to be very small compared to the uncooled 6-inch RDE, it was successfully run for several 20 second periods. The fuel supply system frequently caused drops in the hydrogen flow rate during the engine operation, but the steadiest run started with a total mass flow rate of 220 lb/min and an equivalence ratio of 1.08 and showed 141 kW of heat into the outer wall and 409 kW into the inner wall. This corresponded to an average heat flux into the outer wall of 2.2 MW/m^2. This is low compared to the 8 MW/m^2 seen from the heat flux gauge in the uncooled RDE but it implies, along with problems with cooling this region to thermal equilibrium, that the region with the greatest heat flux is near the base of the detonation channel.

Heat flux into the inner wall is much more difficult to calculate since the center body absorbed heat from both the detonation channel and the exhaust plume. Assuming the detonation channel was the only source of heat, the inner wall averaged 6.7 MW/m^2. Assuming an even distribution over the entire exposed surface area of the center body, the heat flux into the inner wall averaged 5.0 MW/m^2. If the heat was only greater into the center body due to the increased conductivity of the steel wall, it should have seen a heat flux of 4.4 MW/m^2, implying the exhaust plume provided greater heat transfer than the detonation waves in the channel.

The water-cooled RDE also revealed that the assumption that a mild steel center body would absorb 5% of HHV is low, but was not far off from the recorded 6.1%. As a percentage of LHV, the 7.1% absorbed by the 6-inch center body matches nicely with the 8% of measured enthalpy absorbed by the 3-inch center body. Although the water-cooled 6-inch RDE center body saw more heat than what it was designed for, the design was robust enough that the increase was not enough to prevent steady operation. Meanwhile, 5% of either HHV or LHV proved greater than necessary for the stainless steel outer body, which saw only 56% of the design heat rate. While this much overdesign certainly allows for continuous operation, future RDE designs may have restrictions on weight or water flow rates which would make overdesigning the heat exchanger impractical

5.2 Recommendations for Future Water-Cooled RDE Research

In order to operate the cooled RDE longer than 20 seconds, the poor venting of the exhaust in the current setup needs to be addressed. An aluminum shield would help reduce heating of the room by the plume, but would interfere with real-time visual inspection of the plume to determine detonations. Blowing mixing air from behind the RDE is viable, but may not be enough to force air out of the test cell. Another option would be to place another detection thermocouple higher above the engine to detect if the heat continues to rise or if there is a height that is unaffected by the engine operation.

One of the most important next steps is to map the RDE operating space. This is done by attempting to start the RDE at a large number of flow rates and equivalence ratios and establishing which regions allow successful detonation and which regions inhibit successful detonations. A complete operating map will allow other operators to

start the RDE without testing a wide range of operating points each time the RDE is tested. Current research suggests that this RDE's initial operating map is not very large.

On the topic of operating maps, AFRL recently tested an RDE with the same size detonation channel as the 6-inch RDE but a significantly modified injection scheme. This RDE was able to detonate at a much broader operating range than the 6-inch RDE (4). This suggests that if the fuel and air manifolds in the cooled RDE could be modified to allow better mixing, its operating map could be vastly expanded. The two steps to evenly distribute fuel through the fuel manifold mentioned in chapter 4, increasing the number of fuel inlets and adding another stagnation plate, should be implemented one at a time to measure the improvement of each modification individually. These steps could also be applied to the air flow entering the detonation channel.

Another approach to increasing the operating space may be to force the fuel flow to drop after startup. More tests should be done to observe the effects of decreasing equivalence ratio after start-up to confirm the detonation continues and to establish the minimum flow rates that can be used while maintaining detonation activity. In other words, a "post-ignition" operating map should be made to compare to the startup-only operating space. This could be done by requesting fuel or air upstream pressures that stay constant for a certain interval before changing to a new value to maintain for another interval. This ramp and plateau pressure profile would allow for higher certainty in the mass flow rate for a given pressure by allowing the flow upstream to reach equilibrium and by allowing the RDE to reach thermal equilibrium at each flow regime. The cooled RDE is in a good position to test this, as its long operating time enables it to reach thermal equilibrium several times in a single run. This should be done both before and

after any further modifications to the fuel and air manifolds to see if the improved stability during operation is affected by the changes.

Additional topics for this RDE could include incorporating a back-pressurization device, which has been shown in the uncooled 6-inch RDE to increase its operating space. It would be interesting to see if back pressurization only improves initial detonability of a mixture or if it would also allow for lower equivalence ratios after startup. Modification for other fuels might be as simple as changing the fuel plate. A more interesting use of this RDE in investigating other fuels would be to detonate a hydrogen-air mixture, then slowly replace the hydrogen with a less detonable fuel in an effort to run an RDE on different fuel supplies. This is normally impossible on uncooled designs due to the long operating time needed to make a steady transition, but the cooled RDE would be capable of slow and deliberate transitions. This would require significant infrastructure modification to allow two fuel sources, and should be done after investigating the post-ignition operating map to help understand how best to transition between fuels.

5.3 Recommendations for Future Heat Flux Gauge Research

Further work should also be done regarding the heat flux gauge measurements. Several gauges may still be reparable enough to attempt different sealing solutions in the fillet of the gauge. High-temperature RTV paste is used to seal pressure sensors on the RDEs at the DERF, and may be enough to absorb pressure waves and stop detonation gasses from escaping through the heat flux gauge, but will likely erode just as quickly as other materials. Assuming another gauge can be repaired, it should be tested at lower mass flow rates and equivalence ratios in order to characterize steady flow wave

functions. If several could be repaired, measuring up to five gauges during a single run could provide a convincing heat flux profile along the height of the channel.

The digitization-level noise in the gauge signal can be reduced by increasing the gain applied to the signal. Furthermore, it is possible to construct a circuit which would cause the initial voltage to drift to zero. This would increase the signal to resolution ratio, reducing the digitization-level noise to signal ratio and vastly improving the signal to noise ratio of the heat flux gauge signal.

One thing that would have greatly improved the ability to confirm if each waveform on the heat flux gauge corresponded to a detonation would be top-down high-speed video of the channel. Such a setup is already in place for the 6-inch RDE, but was neglected because it was believed that the PCB would serve this function well enough. High-speed video would show not only the timing of each wave but also the intensity and what sort of detonation operation the RDE was undergoing throughout the run. For the run tested, it would have served to confirm or refute the interpretation from the PCB that the RDE established steady 2-wave operation.

The ultimate extension of the heat flux gauge would be to install a high-density platinum RTD array like those designed for turbine instrumentation. The primary concern is the array's ability to stay attached to the containing wall in an environment where ablation is a common occurrence. If the array can survive in the detonation channel the high spatial and temporal resolution afforded would be invaluable in understanding the science of rotating detonation waves, as nearly all models currently available are computer generated.

APPENDIX A. 20-SECOND COOLED RDE RUNS

The cooled 6-inch RDE was run four times for 20 seconds each. However, none of the runs maintained a constant mixture composition for the entire 20 seconds. Moreover, the noise from the thermocouples was so bad that the calculation of instantaneous heat rates gave no useful information. Instead, a moving average of each temperature trace was used to calculate heat flux to see if heat flux leveled off. Since the steadiest run, 144710, only maintained steady equivalence ratio for 10 seconds and thermal equilibrium was reached sometime around 2 seconds after ignition, an 8 second average could be used to find the heat rates for that run. In order to allow the RDE a buffer to reach thermal equilibrium, this period was reduced to a 5 second average. Since 5 seconds corresponds to 5000 samples, the moving averages were made with 5000 sample intervals. The following figures show the moving averages for each run, along with the air flow rates, which were constant for each run, and equivalence ratios, which were not.

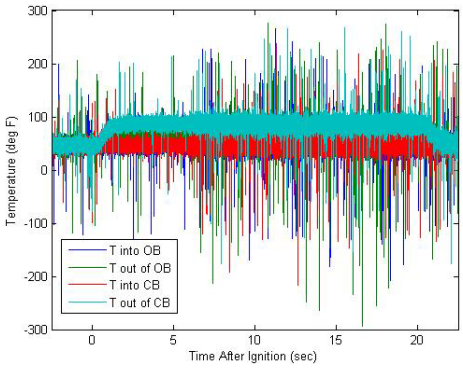

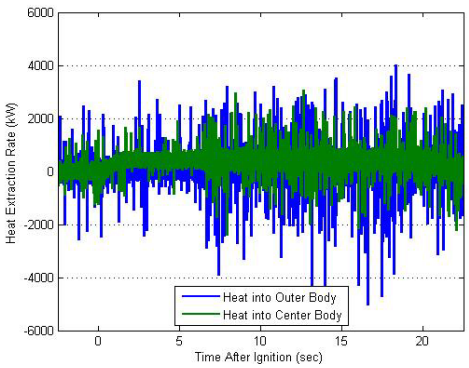

Raw temperature data (left) and heat rates calculated using raw temperature data (right). Specific heat and density were still calculated using 5000 sample averages.

Run 141910:

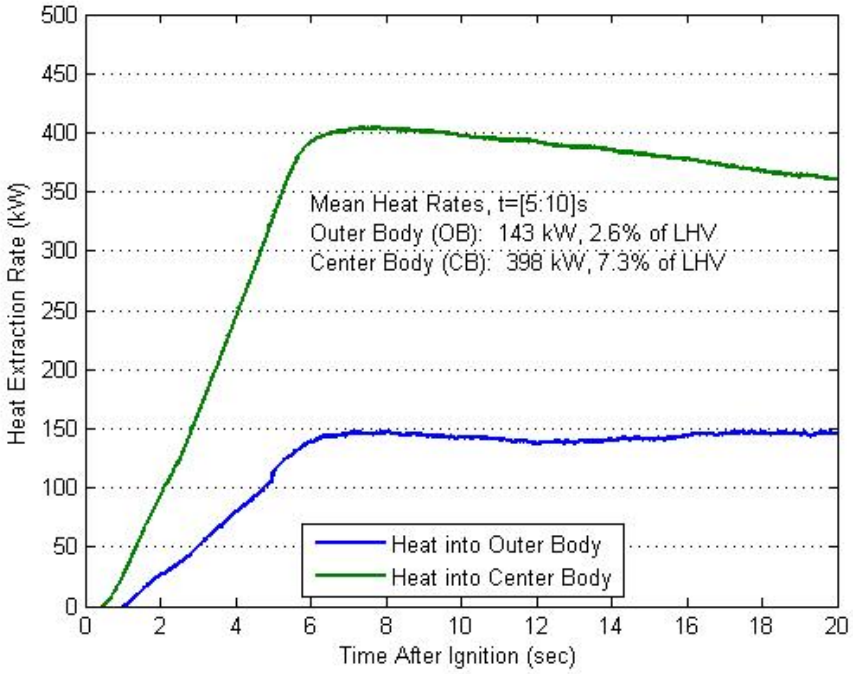
Mean Heat Rates, t=[5:10]s
Outer Body (OB): 143 kW, 2.6% of LHV
Center Body (CB): 398 kW, 7.3% of LHV
Heat into Outer Body
Heat into Center Body
Heat Extraction Rate (kW)
Time After Ignition (sec)

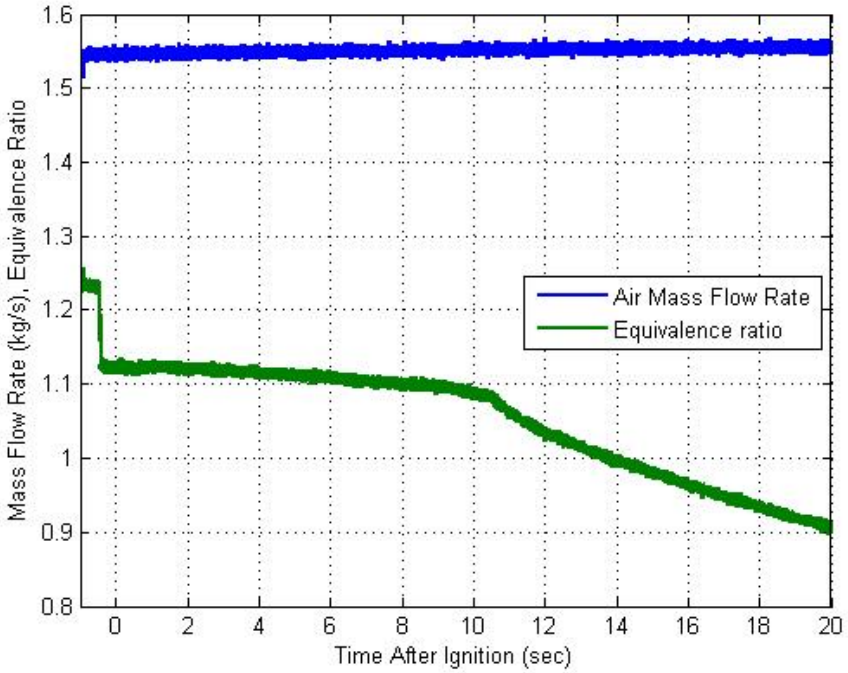
Air Mass Flow Rate
Equivalence ratio
Mass Flow Rate (kg/s), Equivalence Ratio
Time After Ignition (sec)

Run 144717:

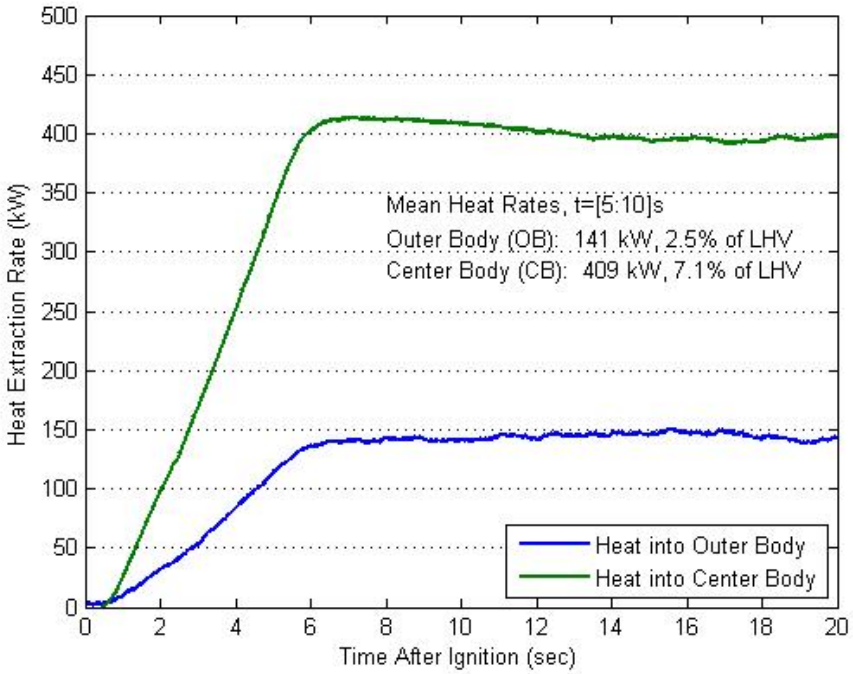
Mean Heat Rates, t=[5:10]s
Outer Body (OB): 141 kW, 2.5% of LHV
Center Body (CB): 409 kW, 7.1% of LHV
Heat into Outer Body
Heat into Center Body
Heat Extraction Rate (kW)
Time After Ignition (sec)

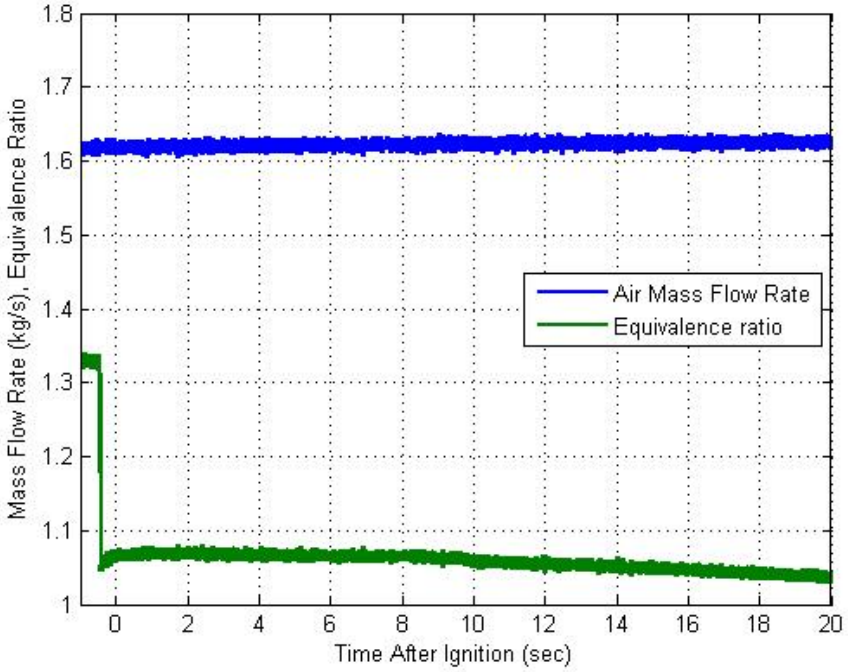
Air Mass Flow Rate
Equivalence ratio
Mass Flow Rate (kg/s), Equivalence Ratio
Time After Ignition (sec)

Run 145210:

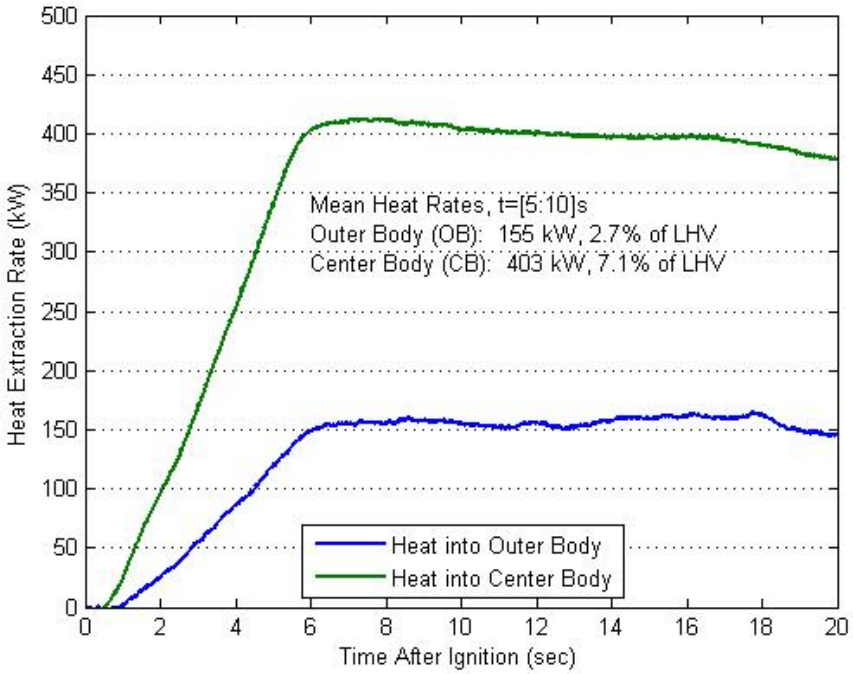
Mean Heat Rates, t=[5:10]s
Outer Body (OB): 155 kW, 2.7% of LHV
Center Body (CB): 403 kW, 7.1% of LHV
Heat into Outer Body
Heat into Center Body
Heat Extraction Rate (kW)
Time After Ignition (sec)

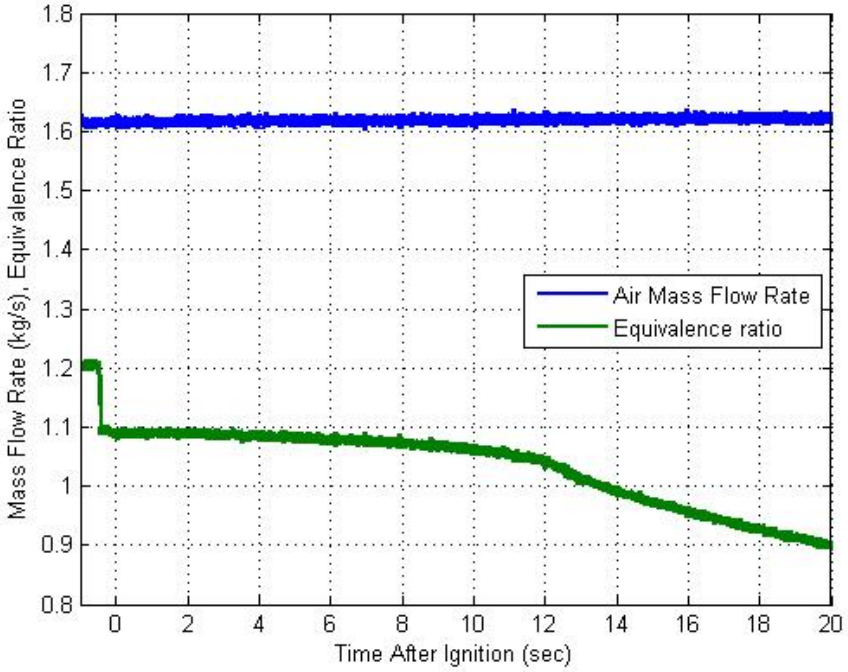
Air Mass Flow Rate
Equivalence ratio
Mass Flow Rate (kg/s), Equivalence Ratio
Time After Ignition (sec)

Run 153348 (Fig. 11 and Fig. 19 came from the start and end of this run):

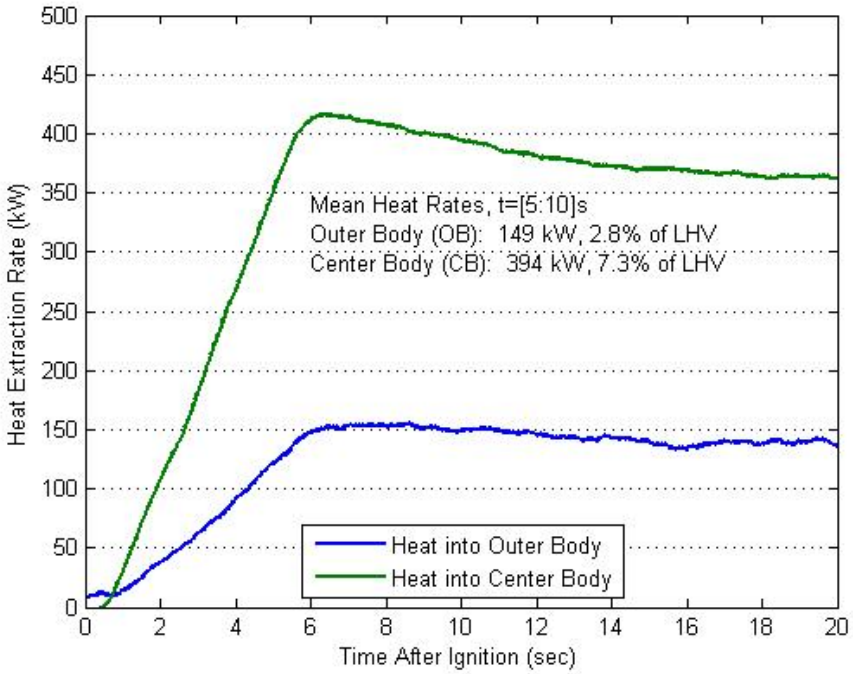

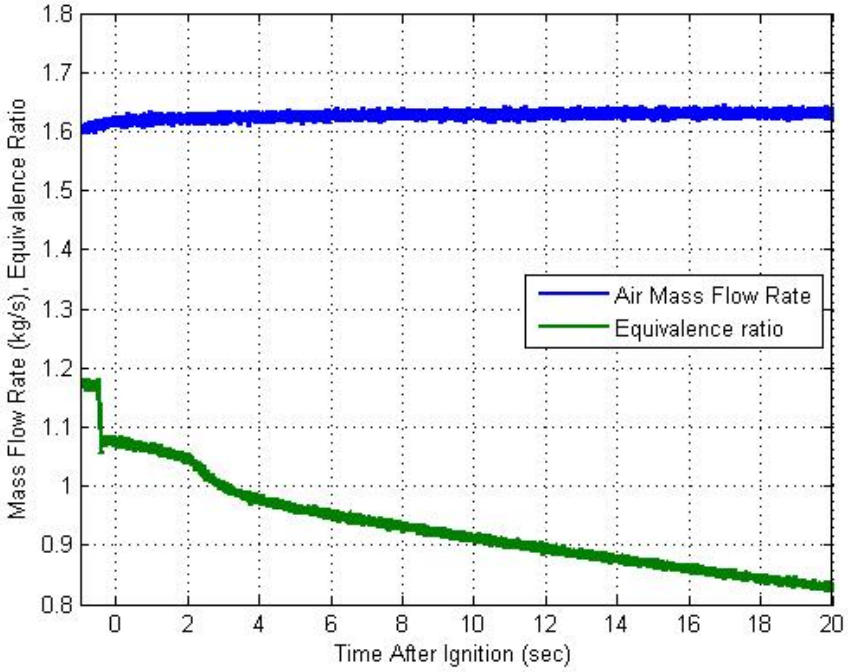

APPENDIX B. COOLED RDE REASSEMBLY

The following figures represent the steps taken to reassemble the cooled RDE after modifying the fuel spacer and the outer body. In the starting state the 0.75” base plate and 1.65” air spacer are bolted to the engine mount. The back plate with the fuel and center body water hoses is loosely bolted to the back plate.

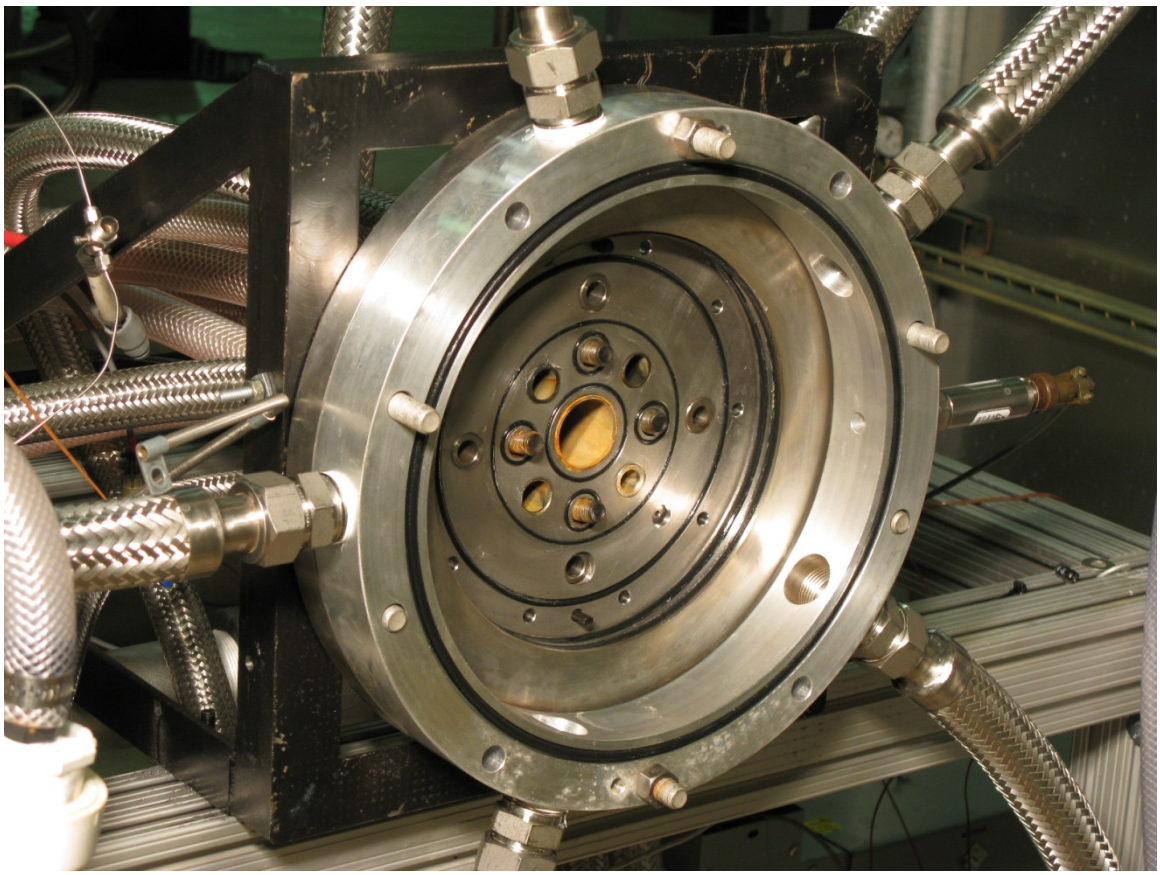

Next the modified fuel spacer is bolted to the back plate and the back plate is firmly bolted to the base plate. The water spacer in the center is also set in place.

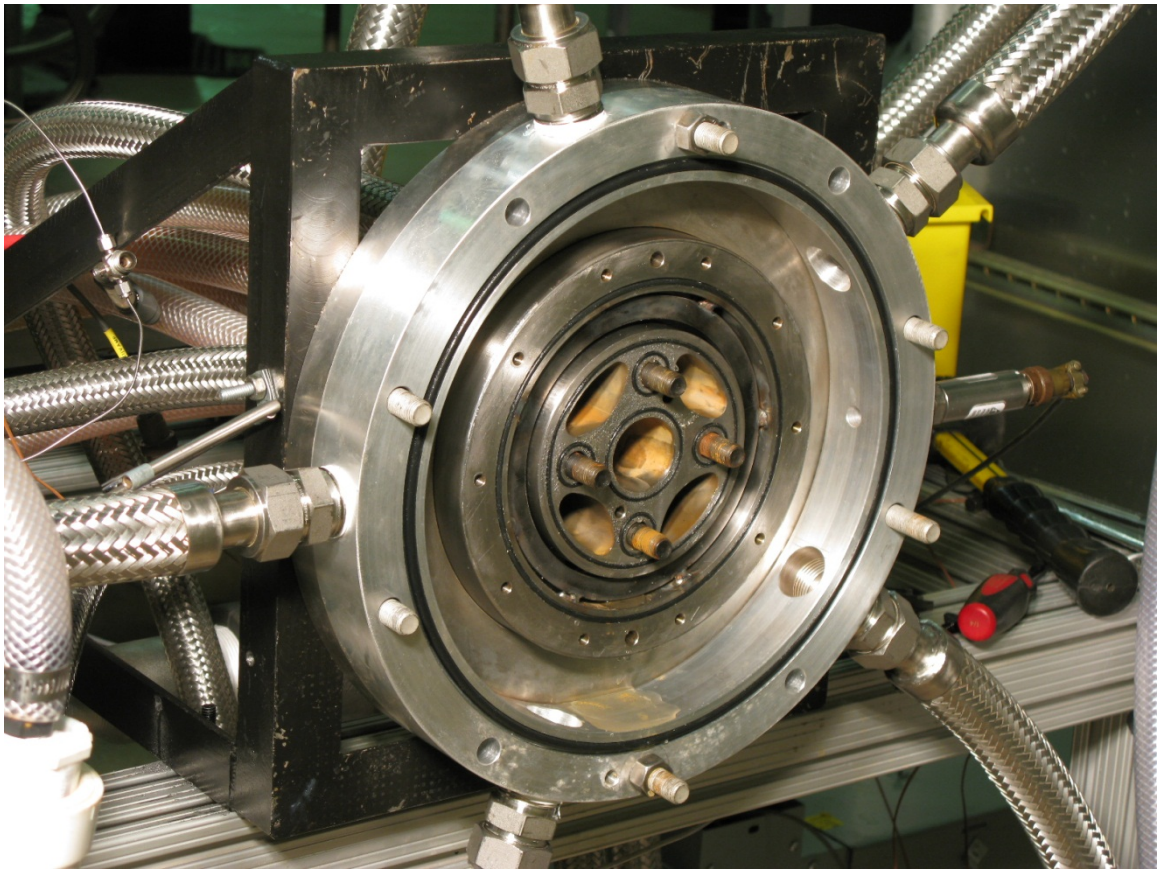

The fuel plate is then bolted onto the fuel spacer. Pins guide the water spacer into position beneath the fuel plate.

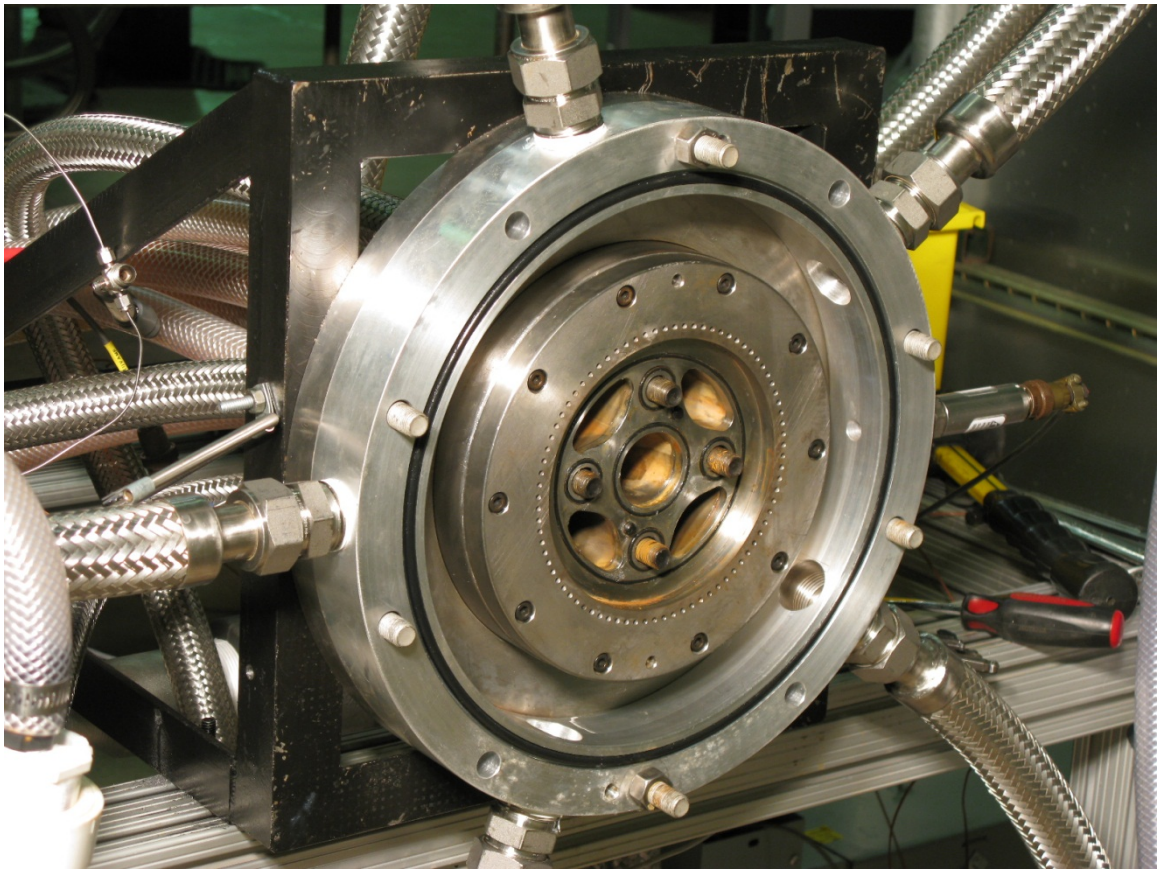

Next the center body is bolted to the fuel plate, fitting 0.300” beneath the exit plane of the fuel plate.

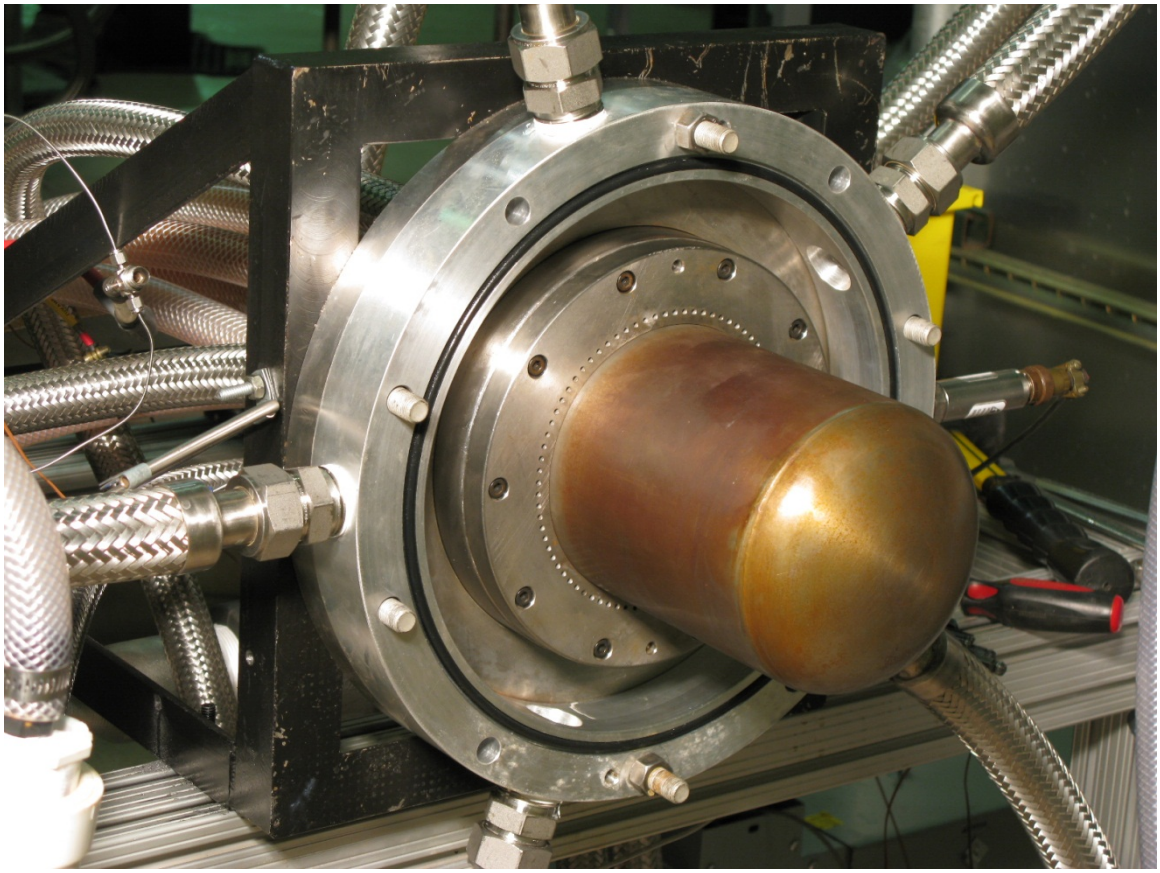

With the center assembly finished, the now one-piece outer body is bolted to the air spacer. The pre-detonator is also affixed to the outer body and its mounting clamps are tightened to prevent movement during operation.

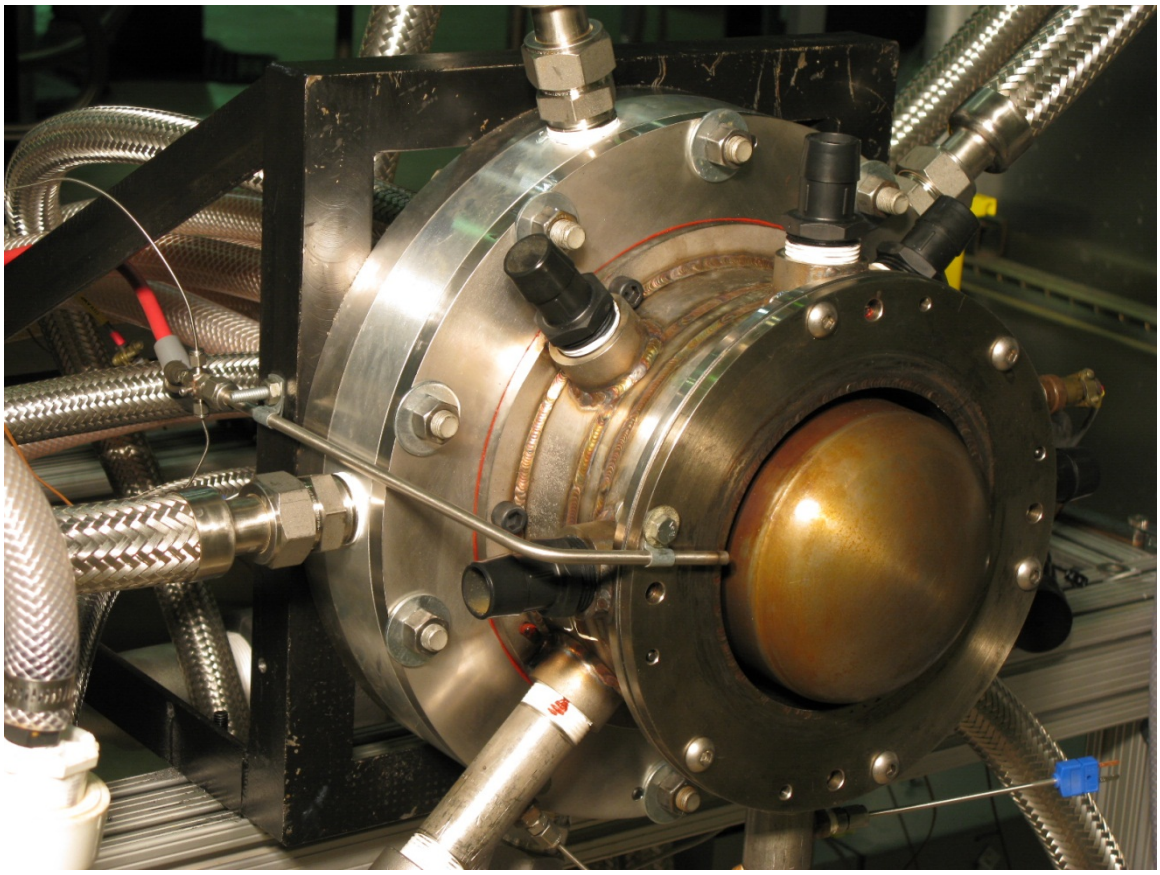

After attaching water lines, the RDE is fully assembled.

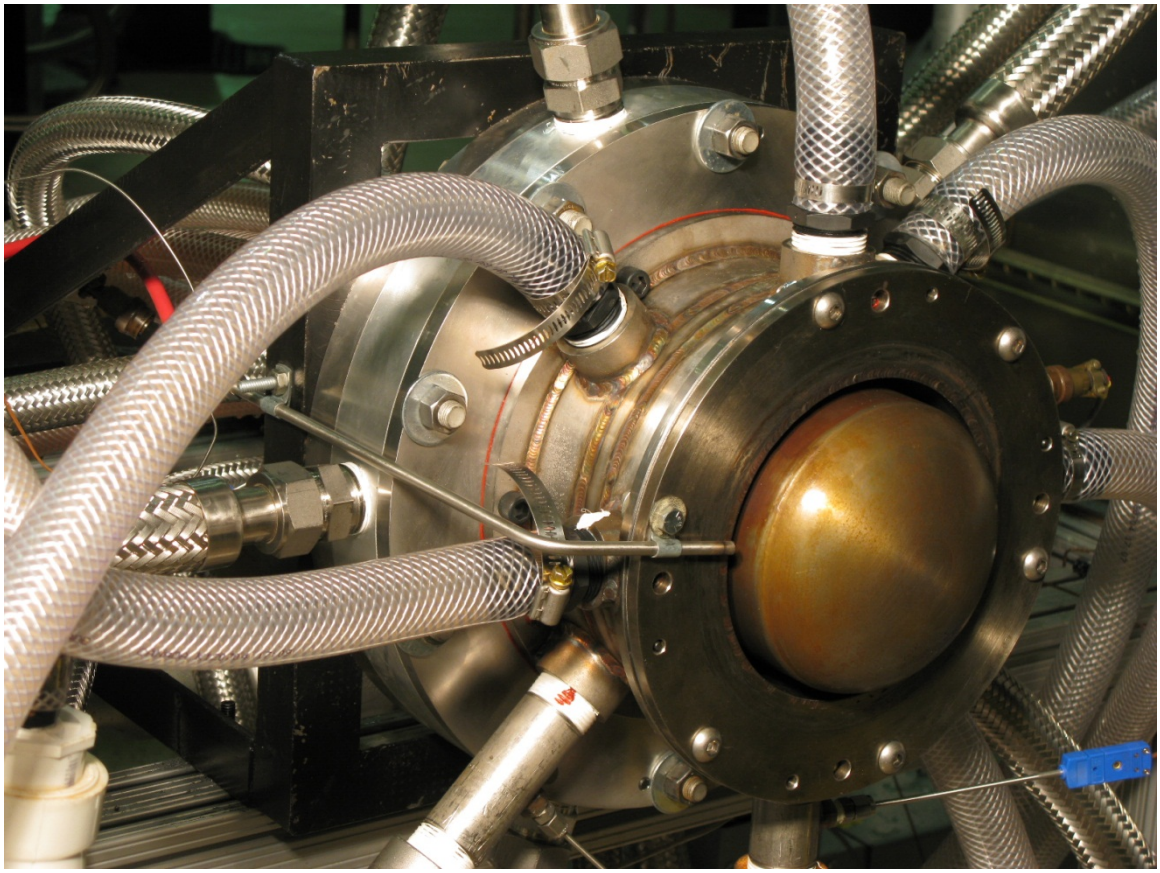

REFERENCES

1. Paxton, Daniel E., Andrew G. Naples, John L. Hoke, and Fred Schauer. "Numerical Analysis of a Pulse Detonation Cross Flow Heat Load Experiment," *49th AIAA Aerospace Sciences Meeting*. Orlando, FL, January 2011.

2. Shank, Jason C. *Development and Testing of a Rotating Detonation Engine Run on Hydrogen and Air.* MS Thesis, AFIT/GAE/ENY/12-M36. Graduate School of Engineering and Management, Air Force Institute of Technology (AU). Wright-Patterson AFB OH, March 2012.

3. Russo, Rachel M. *Operational Characteristics of a Rotating Detonation Engine Using Hydrogen and Air.* MS Thesis, AFIT/GAE/ENY/11-J03. Graduate School of Engineering and Management, Air Force Institute of Technology (AU). Wright-Patterson AFB OH, June 2011.

4. Naples, Andrew, John Hoke, James Karnesky, and Fred Schauer. "Flowfield Characterization of a Rotating Detonation Engine," *51st AIAA Aerospace Sciences Meeting*. Dallas, TX, January 2013.

5. Naples, Andrew G. Engineer, Innovative Scientific Solutions Inc., Dayton OH. Personal Correspondence. June 2012-February 2013.

6. Shank, Jason C., Paul I. King, James Karnesky, Frederick R. Schauer, and John L. Hoke. "Development and Testing of a Modular Rotating Detonation Engine," *50th AIAA Aerospace Sciences Meeting*. Nashville, TN, January 2012. AIAA 2012-0120

7. Anthony, R. J., J. P. Clark, S. W. Kennedy, J. M. Finnegan, P. D. Johnson, J. Hendershot, and J. Downs. "Flexible Non-Intrusive Heat Flux Instrumentation on the AFRL Research Turbine," *ASME Turbo Expo 2011*. Vancouver, Canada, June 2011. GT2011-46853.

8. Oldfield, M. L. G. "Impulse Response Processing of Transient Heat Transfer Gauge Signals," *Journal of Turbomachinery*, 130 (2008).

9. Turns, Stephen R**.** *An Introduction to Combustion: Concepts and Applications.* (2nd Edition). Boston: McGraw-Hill, 2000.

10. Bergman, Theodore L., Adrienne S. Lavine, Frank P. Incropera, and David P. Dewitt. *Fundamentals of Heat and Mass Transfer.* Hoboken: John Wiley & Sons, Inc., 2011.

11. Çengel, Yunus A. and Robert H. Turner. *Fundamentals of Thermal-Fluid Sciences.* New York: McGraw-Hill, 2001.

12. Hibbeler, R. C. *Mechanics of Materials.* 7th. Upper Saddle River : Pearson Prentice Hall, 2008.

13. Bykovskii, F. A. and E. F. Vedernikov. "Heat Fluxes to Combustor Walls during Continuous Spin Detonation of Fuel-Air Mixtures," *Combustion, Explosion, and Shock Waves*, 44: 70-77 (2009)

REPORT DOCUMENTATION PAGE

Form Approved
OMB No. 074-0188

The public reporting burden for this collection of information is estimated to average 1 hour per response, including the time for reviewing instructions, searching existing data sources, gathering and maintaining the data needed, and completing and reviewing the collection of information. Send comments regarding this burden estimate or any other aspect of the collection of information, including suggestions for reducing this burden to Department of Defense, Washington Headquarters Services, Directorate for Information Operations and Reports (0704-0188), 1215 Jefferson Davis Highway, Suite 1204, Arlington, VA 22202-4302. Respondents should be aware that notwithstanding any other provision of law, no person shall be subject to an penalty for failing to comply with a collection of information if it does not display a currently valid OMB control number.
PLEASE DO NOT RETURN YOUR FORM TO THE ABOVE ADDRESS.

1. REPORT DATE *(DD-MM-YYYY)*	2. REPORT TYPE	3. DATES COVERED *(From – To)*
21-03-2013	Master's Thesis	MAR 2012 – MAR 2013

TITLE AND SUBTITLE

Heat Exchanger Design And Testing for a 6-Inch Rotating Detonation Engine

5a. CONTRACT NUMBER

5b. GRANT NUMBER

5c. PROGRAM ELEMENT NUMBER

6. AUTHOR(S)

Theuerkauf, Scott W., 2nd Lieutenant, USAF

5d. PROJECT NUMBER

5e. TASK NUMBER

5f. WORK UNIT NUMBER

7. PERFORMING ORGANIZATION NAMES(S) AND ADDRESS(S)

Air Force Institute of Technology
Graduate School of Engineering and Management (AFIT/ENY)
2950 Hobson Way, Building 640
WPAFB OH 45433-8865

8. PERFORMING ORGANIZATION REPORT NUMBER

AFIT-ENY-13-M-33

9. SPONSORING/MONITORING AGENCY NAME(S) AND ADDRESS(ES)

Attn: Dr. Frederick Schauer
Air Force Research Laboratory
Aerospace Systems Directorate, Turbine Engine Division, Combustion Branch, Advanced Concepts Group
Bldg 71A, D-Bay, 7th St.
Wright Patterson AFB, OH 45433-7251
DSN 785-6462, frederick.schauer@wpafb.af.mil

10. SPONSOR/MONITOR'S ACRONYM(S)

AFRL/RQTC

11. SPONSOR/MONITOR'S REPORT NUMBER(S)

12. DISTRIBUTION/AVAILABILITY STATEMENT

APPROVED FOR PUBLIC RELEASE; DISTRIBUTION UNLIMITED.

13. SUPPLEMENTARY NOTES

This material is declared a work of the U.S. Government and is not subject to copyright protection in the United States.

14. ABSTRACT

This thesis explains the design and testing of a water-cooled rotating detonation engine (RDE) run on hydrogen and air. The change in water temperature as it cooled the engine was used to find the steady heat rate into the containing walls of the detonation channel. The engine successfully ran four times for 20 seconds each. The steady-state heat rate was measured to be 2.5% of the propellant lower heating value (LHV) into the outer wall and 7.1% of LHV into the inner wall. Additionally, a quick-response resistance temperature detector (RTD) was used in an uncooled RDE of similar dimension to the cooled RDE to estimate the transient heat flux profile in the detonation channel. The average heat flux into the outer wall near the base of the channel was measured to be four times greater than the average heat flux over the entire cooled wall at steady-state, indicating the heat flux decreases significantly with axial distance. In addition, the large difference in heat absorption between the inner and outer cooled walls indicates that the heat flux into the inner wall is greater than that into the outer wall.

15. SUBJECT TERMS

Detonation, RDE, Cooled, Heat, Combustion, RTD, Transient

16. SECURITY CLASSIFICATION OF:			17. LIMITATION OF ABSTRACT	18. NUMBER OF PAGES	19a. NAME OF RESPONSIBLE PERSON
a. REPORT	b. ABSTRACT	c. THIS PAGE			King, Paul I., Civ, USAF ADVISOR
U	U	U	UU	79	19b. TELEPHONE NUMBER *(Include area code)* (937)255-3636, ext 4628 paul.king@afit.edu

Standard Form 298 (Rev. 8-98)
Prescribed by ANSI Std. Z39-18